Molecular Dynamics of Heat Transfer Liquids of Complex Rheology

Yunes Salman
City, University of London
Department of Mechanical Engineering and Aeronautics

Supervised by
Dr. Ioannis Karathanasis
Prof. Dr. Manolis Gavaises

A thesis submitted for the degree of
Master of Philosophy (MPhil)
March 2023

Abstract

Electric car batteries generate substantial heat during operation, requiring efficient heat dissipation to maintain battery performance and longevity. Nanofluids, suspensions of nanoparticles in a fluid base, have emerged as promising solutions for effective cooling systems due to their enhanced thermal conductivity and improved properties. This thesis investigates the potential of nanofluids for electric car battery cooling systems using Molecular Dynamics (MD) simulations to study nanofluid behaviour at the atomistic level. By examining the thermal and rheological properties of nanofluids, MD simulations provide valuable insights into the design and optimisation of heat transfer fluids for electric car battery cooling systems. Results from the simulations show significant thermal conductivity enhancement in polyalphaolefin (PAO)-2/Cu and PAO-2/Ag nanofluids, indicating their potential for use in Battery Thermal Management Systems (BTMS). This study not only advances our understanding of nanofluids, but also contributes to the development of more efficient and sustainable electric vehicle battery cooling technologies.

Acknowledgement

I would like to express my deepest gratitude to my supervisors, Prof. Manolis Gavaises, and Dr. Ioannis Karathanasis, for their support, guidance, and mentorship throughout my research journey. Their expertise, enthusiasm, and encouragement have been invaluable in shaping my work. I feel incredibly fortunate to have had the opportunity to work under their supervision.

I also wish to extend my heartfelt thanks to my colleagues and friends at the City, University of London, who have contributed to my personal and professional development in many ways. I would like to give special thanks to my dear friend and colleague Bharath Ravikumar, who helped me countless times with discussions and brainstorming.

To my incredible parents, I want to extend a heartfelt thank you for instilling within me the core values of hard work and perseverance. Your guidance and nurturing of my curiosity and passion for learning have shaped me into the person I am today. I am truly fortunate to have you as my role models. To my siblings, thank you for your constant encouragement and for always being there for me, and for proofreading this thesis!

I want to express my love to each and every one of you. You have been my pillars of support throughout this journey, and I am eternally grateful for your presence in my life.

Table of Contents

List of Figures

List of Tables

List of Abbreviations and Symbols

Å	Angstrom
bf	Base fluid
k_b	Boltzmann constant, 1.38 × 10-23 J/K
cSt	Centistoke
ϕ	Cut-off radius
ρ	Density
ε	Depth of the potential well (J)
r_{ij}	Distance between two interacting particles
F	Force
η	Fricition coefficient
J	Heat flux
σ	Interatomic length scale (nm)
m	Mass
mm2 s^{-1}	Millimetres per second
Λ	Mean free path
nm	Nanometres
np	Nanoparticle
M	Number of integration steps
N	Number of simulation steps
C	Specific heat per unit volume
T	Temperature
$\frac{\partial T}{\partial x}$	Temperature gradient
$\lambda_{\mu v}$	Thermal conductivity tensor
t	Time
v	Velocity
μ	Viscosity

AMBER	Assisted Model Building with Energy Refinement
Ar	Argon
BTMS	Battery Thermal Management System
C20H42	9,10-Dimethyloctadecane
CFD	Computational Fluid Dynamics
CHARMM	Chemistry At Harvard Molecular Mechanics
Cu	Copper
EAM	Embedded atom model

EMD	Equilibrium Molecular Dynamics
EV	Electric Vehicle
FCC	Face-Centered Cubic
GROMACS	Groningen Machine for Chemical Simulations
HCACF	Heat Current Autocorrelation Function
LAMMPS	Large-Scale Atomic/Molecular Massively Parallel Simulator
LJ	Lennard-Jones
LL	Liquid liquid interaction
L-OPLS-AA	Ligand Optimized Potential Energy Surface All-Atom
MC	Monte Carlos
MD	Molecular Dynamics
NAMD	Nanoscale Molecular Dynamics
NEMD	Non-Equilibrium Molecular Dynamics
NPT	Isothermal–isobaric ensemble. Constant number of particles (N), pressure (P), and temperature (T)
NVE	Microcanonical ensemble. Constant number of particles (N), volume (V), and energy (E)
NVT	Canonical ensemble. Constant number of particles (N), volume (V), and temperature (T)
PAO	Polyalphaolefin
QM	Quantum Mechanics
SL	Solid liquid interaction
SS	Solid solid interaction
TIMs	Thermal Interface Materials
VMD	Visual Molecular Dynamics

1. Introduction

The thermal conductivity of a material is a measure of its ability to transfer heat, and it is an important property for the heat transfer liquids of electric car batteries, as it directly affects the efficiency of the cooling system. The high energy density of the batteries in electric cars generates high levels of heat during operation, and this heat must be dissipated effectively to maintain the performance and longevity of the battery.

The thermal conductivity of the materials used in the cooling system, such as the heat transfer fluid and the thermal interface materials (TIMs) between the battery cells and the cooling system, plays a crucial role in the effectiveness of the cooling system. High thermal conductivity materials are able to transfer heat more effectively and therefore cool the battery more efficiently. Thus, there is a crucial need to design heat transfer fluids with high thermal conductivity. Fortunately, nanofluids have been studied intensively for around 30 years and are the best solution to this problem.

Nanofluids are suspensions of nanoparticles in a fluid base, such as water or an organic liquid. Nanoparticles, which are typically in the size range of 1-100 nanometres, can be made from a variety of materials, including metals, metal oxides, and carbon-based materials. The use of nanoparticles in a base fluid leads to unique properties that are not found in bulk materials, such as enhanced thermal conductivity, increased stability, and improved optical properties.

One of the most well-studied properties of nanofluids is their enhanced thermal conductivity. The addition of nanoparticles to a base fluid leads to an increase in the overall thermal conductivity of the fluid, which can be attributed to both the increase in the number of heat-carrying phonons in the fluid and the increased convective heat transfer due to the increased fluid viscosity caused by the nanoparticles. The enhancement of thermal conductivity is dependent on the type and concentration of nanoparticles, as well as the base fluid choice.

In addition to enhanced thermal conductivity, nanofluids also exhibit improved stability compared to suspensions of larger particles. The small size of the nanoparticles leads to a high surface area-to-volume ratio, which makes them less likely to settle out of the base fluid. This improved stability allows for the use of nanofluids in applications where suspensions of larger particles would not be practical.

Nanofluids have been proposed for a wide range of applications, including heat transfer, thermal energy storage, and biomedical applications. Some of the most promising applications include the use of nanofluids as coolants in electronic devices, as heat transfer fluids in solar thermal systems, and as a means of enhancing the efficiency of cooling towers in power plants.

Advancements in nanotechnology made the production of nanoparticles made of metals, oxides, and carbides possible. There are various techniques used to create these particles, including chemical and vapour deposition, arrested precipitation, sonication, and pulsed laser vaporisation. Nanofluids, a type of solid-liquid suspension, hold potential in improving energy-efficient heat transfer. These fluids contain metal or oxide nanoparticles suspended in a base fluid and can enhance the thermal conductivity of the fluid. Nanofluids have the potential to improve the performance of heat exchangers and cooling devices, which are important for industries like automotive and aerospace, as they work towards reducing the weight of thermal management systems. This is specifically desired in electrical car batteries thermal management systems.

To that end, new cooling concepts are being explored that focus on using heat transfer liquids with customised properties for the specific application, instead of using traditional coolants like water or air [1]. Which is why the Battery Thermal Management System (BTMS) is used to regulate the temperature of a battery pack in an electric vehicle (EV). The system helps to maintain optimal battery temperature for improved performance, extended battery life, and safe operation. BTMS typically includes cooling or heating elements, temperature sensors, and a control system. The aim of BTMS is to keep the battery temperature within a safe and efficient operating range, regardless of external temperature conditions. This leads to increasing the lifetime of the battery [2]. The problem with BTMS is that current research is limited and fragmented across various cooling techniques, each with their own limitations. For example, single-phase forced convection does not provide the necessary cooling efficiency, convective flow-boiling requires a large quantity of cooling liquid, and pool-boiling is not sustainable for multiple cycles [3]. This results in a need for a more effective and efficient cooling solution for BTMS. A proposed solution is to use single-phase immersion cooling with dielectric liquids to cool electric vehicle components [4], specifically the battery pack, without the need for excessive pumping and large heat exchangers.

Novel dielectric coolant fluids are a class of cooling liquids that have unique electrical properties. They are being developed as a solution to the limitations of conventional cooling fluids, such as water, that are often used in cooling systems [4]. The primary objective of using these fluids is to improve the heat transfer processes in future BTMS (heat exchangers), which are essential components of many cooling systems. Heat transfer processes in heat exchangers occur through the transfer of heat from one fluid to another. The effectiveness of this process is determined by several factors, including the properties of the fluids involved and the design of the heat exchanger itself.

One of the key properties of the fluid is its rheology, which relates to the flow behaviour of the fluid and its ability to transfer heat. The identification of rheological properties capable of enhancing the underlying heat transfer processes is expected to maximise the effectiveness of future BTMS. This is because the rheology of a fluid can significantly impact its ability to transfer heat. For example, fluids with high viscosity will have a slower flow rate and will therefore be less effective at transferring heat than fluids with low viscosity.

One of the main advantages of using novel dielectric coolant fluids is that they have a high thermal conductivity, which allows for efficient heat transfer. Additionally, these fluids are non-conductive and non-corrosive, which makes them safe to use in a variety of applications. This also eliminates the risk of electrical or chemical damage to the components of the cooling system. Another important advantage of these fluids is their low vapour pressure, which means that they do not boil or evaporate easily. This makes them ideal for use in high-temperature applications, where conventional cooling fluids may not be suitable. Additionally, they are also non-toxic, which makes them safe for use in applications where human contact is a concern. The identification of the rheological properties of these fluids is critical to their effectiveness in improving heat transfer processes in future BTMS. This involves characterising the fluid's flow behaviour under different conditions, such as temperature and pressure, and measuring its thermal conductivity, viscosity, and density.

Enhancing thermal conductivity on nanofluids is crucial for improving the performance and safety of BTMS. It efficiently dissipates heat generated during battery operation, preventing overheating and ensuring optimal performance, particularly in high-energy-density batteries like those in EVs. This enhancement leads to extended battery life, reduced energy consumption due

to lower operating temperatures, and decreased risks of hotspots. Thermal conductivity enhancement of nanofluids also enables batteries to operate at higher power densities, benefiting applications requiring rapid energy discharge or charging. Additionally, improved thermal conductivity reduces the need for heavy and energy-consuming cooling components, making designs more efficient and lightweight. This not only enables faster charging but also results in cost savings for manufacturers and end-users through longer-lasting batteries and reduced maintenance.

However, novel proposed oil-based fluids with nanoparticle additives [5–7], although showing enhanced thermal properties, their rheology is complicated and displays traits of both liquids and solids when subjected to forces over time, resulting in an unsuitable heat transfer fluid for BTMS for reasons mentioned earlier.

That is why it is important to study nanofluids in more detail, as they are promising enhanced thermal and rheological properties. By designing optimum heat transfer fluids for the mentioned application. To achieve such a goal, Molecular Dynamics (MD) simulation must be used, as it is an excellent tool to study nanofluids on an atomistic scale. MD is a simulation method that uses classical mechanics to model the motion of a large number of particles in a system. This enables the study of the nanofluid behaviour at the molecular level, providing insight into the physical and thermal properties of the nanofluid that cannot be obtained through experiments alone [8–11]. These simulations provide a way to study the behaviour of nanofluids in a controlled environment and observe the thermal, mechanical, and rheological properties of the fluid. They also allow the investigation of the interaction between the fluid and the nanoparticles, the effect of particle size, shape, and concentration on heat transfer, and the formation of nanofluid structures. Also, it can provide a molecular-level understanding of the fluid-particle interactions. This includes the intermolecular forces between the fluid and nanoparticles, and the formation and stability of nanoparticle clusters. These interactions are critical for determining the properties of the nanofluid, and are essential for understanding how these properties can be optimised for specific applications. Another advantage of MD is that it allows researchers to study the behaviour of nanofluids under a wide range of conditions. This is particularly important for the current application of BTMS, where the performance of the nanofluid is highly dependent on the conditions under which it is operating. By using MD simulations, information can be obtained about the complex thermal and transport properties of nanofluids that are difficult or impossible

to obtain experimentally. This information is crucial for optimising the design and performance of nanofluid-based systems, and for understanding the fundamental mechanisms underlying their behaviour.

1.1 Project Goals & Objectives

The primary goal of this project is to investigate the thermal and rheological properties of nanofluids and their potential application in improving heat transfer processes in future BTMS. To achieve this goal, the following specific objectives have been identified:

1. Investigate Thermal and Rheological Properties of Nanofluids:
- Conduct a comprehensive study to understand the thermal conductivity enhancement mechanism of nanofluids.
- Analyse the effect of nanoparticle type, concentration, size, and shape on the thermal and rheological properties of nanofluids.
- Characterize the flow behaviour and viscosity of nanofluids under various temperature and pressure conditions.

2. Improve Heat Transfer Processes in Future BTMS:
- Evaluate the performance of nanofluids in heat transfer applications relevant to BTMS, such as cooling electric vehicle battery packs.
- Determine the optimal nanofluid composition and concentration for efficient heat dissipation and temperature regulation.
- Investigate the feasibility and effectiveness of using nanofluids in different heat exchanger designs for BTMS.

3. Design and Optimise Heat Transfer Fluids for BTMS:
- Develop strategies to tailor the properties of nanofluids for specific BTMS requirements, considering factors such as thermal conductivity, viscosity, stability, and non-toxicity.

- Optimise the composition and concentration of nanoparticles in nanofluids to maximise heat transfer performance, while ensuring long-term stability and compatibility with BTMS components.
- Develop Molecular-Level Understanding through MD Simulations:
- Utilize Molecular Dynamics (MD) simulations to gain insight into the behaviour and interactions of nanofluids at the atomic and molecular scale.
- Investigate fluid-particle interactions, intermolecular forces, nanoparticle clustering, and the formation of nanofluid structures using MD simulations.
- Correlate the findings from MD simulations with experimental data to validate the accuracy and reliability of the simulation results.

4. Provide Insights for Efficient Nanofluid-Based Thermal Management:

- Generate valuable insights into the potential benefits and limitations of nanofluids as heat transfer fluids in BTMS and other thermal management applications.
- Identify key factors and parameters that influence the performance and efficiency of nanofluid-based thermal management systems.
- Propose guidelines and strategies for the effective utilisation of nanofluids to enhance heat transfer efficiency and ensure reliable and safe operation of BTMS.

5. Contribute to Knowledge in Nanofluid Applications:

- Contribute to the existing body of knowledge on nanofluid technology by advancing understanding of nanofluid behaviour and its application in heat transfer systems.
- Publish research findings in peer-reviewed journals and present results at relevant conferences and academic forums to share knowledge with the scientific community.

6. Generate Practical Recommendations for Industry Integration:

- Translate research outcomes into practical recommendations and guidelines for the integration of nanofluid-based thermal management systems in relevant industries, particularly in the automotive and energy sectors.

- Provide insights and recommendations to industry stakeholders regarding the selection, design, and implementation of nanofluids for improved heat transfer in BTMS.
- Foster collaborations with industry partners to facilitate the adoption of nanofluid-based solutions and contribute to the advancement of thermal management technologies.

The project objectives presented above are a comprehensive and ambitious vision for exploring nanofluids and their potential impact on BTMS. However, due to practical constraints, such as limited time and resources, it was necessary to re-evaluate the scope of the project. In section 1.2, a detailed overview will be provided to identify the specific goals and objectives that were successfully achieved. Additionally, a list of the project's accomplishments will be discussed, considering the factors that influenced its scope and limitations. By discussing the achieved milestones and identifying the limiting factors, a comprehensive understanding of the project's outcomes will be presented.

1.2 Project Scope

While MD simulations fundamentally and originally fall under the discipline of Computational Physics or Computational Chemistry, their application in engineering requires additional steps to bridge the gap between simulations and engineering solutions. MD simulations utilise principles from physics, chemistry, and computer science to simulate the behaviour and interactions of atoms and molecules at the atomic scale, offering valuable insights into complex engineering systems.

However, in practice, reaching engineering solutions typically involves multiple stages beyond MD simulations. For instance, in this study, further MD investigations are necessary to explore various nanofluids comprising different nanoparticle materials, concentrations, and sizes. These additional studies would recommend the optimal nanofluid system that exhibits the most favourable thermophysical, thermodynamic, and kinetic properties.

Following this, computational fluid dynamics (CFD) studies would be required to evaluate the recommended nanofluid in a heat exchanger system, examining how it impacts the heat transfer

process. Only through these comprehensive investigations can sound engineering solutions be developed.

Consequently, it is unrealistic to expect definitive engineering solutions from one or two MD studies alone. Rather, MD serves as a valuable tool in engineering, guiding engineers and providing them with insights into the behaviour of the systems they study. This information can be used to inform the design and optimisation of engineering systems, ultimately leading to more effective solutions.

Based on the presented information and the original goals and objectives of this project, the project scope is as follows:

- Investigating one of the thermal properties of nanofluids, namely, thermal conductivity.
- Limited investigation of rheological properties (PAO vs PAO-2).
- How BTMS can benefit from nanofluids with enhanced thermal conductivity.
- Detailed literature review to understand the different MD approaches in studying nanofluids.
- Comparing and choosing the appropriate MD method.
- Utilizing MD simulations to gain insight into the behaviour and interactions of nanofluids at the atomic scale.
- Potential application for PAO-2/Cu & PAO-2/Ag nanofluid.

One of the main limiting factors that changed the original project goals and objectives is the project timeline. Originally, the research proposal of this project was designed for a longer timeline. However, the timeline of the project was cut short.

2. Literature Review

2.1 Introduction

Molecular dynamics (MD) simulations have been widely used in the study of nanofluids, which are suspensions of nanoscale particles in a fluid medium. The literature on the use of MD simulations in nanofluids research spans a wide range of topics. This literature review will focus on the use of MD to study thermal conductivity of nanofluids.

Thermal conductivity of nanofluids refers to the ability of a fluid to transfer heat, and it is an important factor in many industrial and energy applications. Nanofluids, which are suspensions of nanoparticles in a fluid matrix, have been shown to have improved thermal conductivity compared to conventional fluids, making them attractive for use in thermal management systems. The study of thermal conductivity of nanofluids is important, as it can provide valuable information for the design and optimisation of nanofluids for specific applications. However, the complex behaviour of nanofluids, including the interactions between nanoparticles and the fluid matrix, makes it challenging to study their thermal transport properties experimentally. MD simulation provides a powerful tool for the study of thermal conductivity of nanofluids, as it enables the modelling of the motion of individual atoms and molecules in real time. MD simulation can provide detailed information on the mechanism of heat transfer in nanofluids and enable the optimisation of nanofluid design for specific applications, making it an important tool in the field of thermal management.

2.1 Molecular Dynamics

In the 1980s, atomistic descriptions started to get introduced in the modelling of materials by researchers, rather than just using the classical continuum mechanics theories [12]. Atomistic simulations are capable of probing the fundamental behaviour of materials, because it considers the behaviour of the individual particles and assumes they cannot be divided further. They solve systems with a very large number of particles; thus, they cannot be solved analytically, and so computational models are generated instead.

Atomistic simulations are mainly adopted to study the numerous mysterious phenomena and mechanisms that are associated with materials to gain a better understanding of the different processes, its causes and effects, also pursuing the development of the materials and optimising its microstructure. There are many computational and numerical methods that work on an array of different scales, these methods are divided into three sectors; atomistic modelling, continuum modelling and multi-scale modelling. However, the focus of this report is on atomistic modelling.

The main atomistic methods used are the Quantum Mechanics (QM), Monte Carlos (MC) and Molecular Dynamics methods (MD). The MC method deals with complex models where the input is a set of random numbers, and the output is based on the concepts of probability. MD, however, uses the classical equations of motion to evaluate the interactions between the atoms or molecules [13] and it is considered a virtual microscope because of its high spatial and temporal resolution. It is a computational method that simulates the movement of atoms and molecules. MD is the most used method, Alder and Wainwright were first to introduce it, and the details of the approach are presented in their book [14].

a. Initial Assumptions

Due to the complexity of these many particle systems and their interactions, some initial assumptions must be made. The first one is that the nucleus of the atoms is only taken into consideration because the mass of electrons is negligible compared to that of the nucleus. The second one is that there are no changes in the mass of the system at all during the simulation; no atoms are added or removed, and the total kinetic energy is constant. The equations of motions are integrated over a number of time-steps to investigate the behaviour of the position and velocity vectors of each particle.

Thus, the MD method first describes the initial positions and velocities of each atom, and then calculates the forces between them by the interatomic potentials that come from quantum mechanics studies. After that, these initial values are changed by a time interval after calculating the forces, and then these forces are recalculated for the new positions and velocities.

b. Interatomic Potentials

In a MD simulation, the interaction potential can either be bonded or non-bonded. Most non-bonded potentials are represented as pair potentials, which consider the interactions between atoms as one pair at a time. The most commonly used pair potential in molecular dynamics simulations is the Lennard-Jones (LJ) potential. This potential is a 12-6 potential that is attractive when the molecules are far apart, and becomes strongly repulsive when they are close together. The Lennard-Jones potential has an attractive term represented by r6, which represents the van der Waals interaction between atoms at large distances, and a repulsive term represented by r12, which becomes dominant when the atoms come close and represents the resistance to compression between the atoms. The Lennard-Jones pair potential for atoms i and j is given as [17]:

$$\phi_{LJ}(r) = 4\varepsilon\left[\left(\frac{\sigma}{r_{ij}}\right)^{12} - \left(\frac{\sigma}{r_{ij}}\right)^{6}\right] \qquad 2\text{-}1$$

where ε is the depth of the potential well, σ is interatomic length scale, and r_{ij} is distance between two interacting particles.

The expression for the potential energy between two atoms interacting through the Lennard-Jones potential is given by the equation above. It includes two parameters, ε and σ, which determine the depth and shape of the potential curve respectively. ε represents the energy of the potential well and σ represents the distance at which the potential curve crosses the zero line. These parameters can be obtained through quantum chemistry calculations or by fitting the experimental data. The repulsive force, which dominates at short distances, is represented by the r12 part of the potential. The attractive force, which dominates at longer distances, is represented by the r6 part of the potential. The combined potential curve is shown in figure 2-1 .

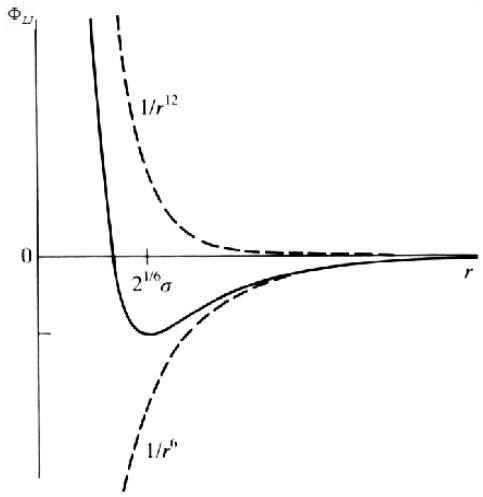

Figure 2-1Potential energy of a particle in LJ model.

Some of the potentials can include the effects of the interactions between three or more atoms, such as the Tersoff potential, which sums the group of atoms taking the angles between them into consideration, and the EAM potential [15–16] which calculates the electron density from the surrounding atoms.

Thus, the reliability of the simulations greatly depends on the chosen potential function.

c. Force Calculation

The force between a pair of atoms is calculated by using the interaction pair potential. This is done by adding up the interactions between atom i and all other atoms in the system. The force on atom i is obtained by taking the derivative of the potential function, as shown in equation 2-1. The interatomic force between two atoms in the Lennard-Jones potential is given by [17]:

$$\vec{f}_{LJ}(r) = \frac{\varepsilon}{r_{ij}}\left[48\left(\frac{\sigma}{r_{ij}}\right)^{12} - 24\left(\frac{\sigma}{r_{ij}}\right)^{6}\right]\widehat{r_{ij}} \qquad 2\text{-}2$$

d. Cut-off Radius

The most time-consuming part of a molecular dynamics simulation is the calculation of forces between atoms, which requires calculating the force on each atom by all other N-1 atoms in the simulation domain at each time step, leading to an $O(N^2)$ growth in computation time. To reduce computation time, a cut-off radius is applied, such that the interaction between atoms outside of a sphere with this radius is ignored. The most commonly used cut-off radius for Lennard-Jones

potential is between 2.5σ and 3.2σ [17]. The Lennard-Jones potential with the cut-off radius implemented is represented as shown in equation 2-1.

$$\phi(r) = \phi_{LJ}(r) - \phi_{LJ}(r_c) \quad \text{if } r \leq r_c$$
$$\phi(r) = 0 \quad \text{if } r > r_c$$

2-3 [17]

e. Verlet Neighbour List

To save computational time in a molecular dynamics simulation, where the calculation of force is the most time-consuming step, a technique called the neighbour list was developed by Verlet [18]. This method creates a list of neighbours for each atom, only considering the atoms in this list when calculating the force on that atom. The neighbour list is updated after a few time steps, such as 10, and takes into account any atoms that may have moved outside the cut-off radius or new atoms that may have entered the radius. To account for this movement, the list is generated using a slightly larger radius, known as r_{list}, where $r_{list} = r_{cut\text{-}off} + \Delta r$.
Figure 2-2 shows the impact of r_{list} on the generation of the neighbour list.

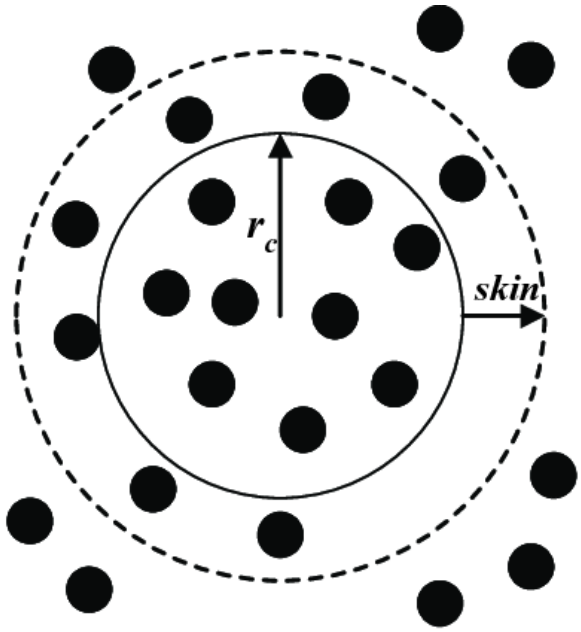

Figure 2-2 Neighbour-list construction with radius rlist [19].

f. Equations of Motion

MD is based on solving the classical Newtonian equations of motion for a system that is interacting through its potential function. Newton's law describes the equation of motion as follows [20]:

$$m_i \frac{\partial^2}{\partial t^2} = F_i \qquad 2\text{-}4$$

where atom i has a force of F, which is described by [20]:

$$F_i = -\nabla_i V(r_{1,\ldots\ldots,} r_N) \qquad 2\text{-}5$$

and the behaviour of the interacting particles is described by the Lagrangian equation [20]:

$$L = \sum_{i=1}^{N} \frac{m\dot{r}^2}{2} \qquad 2\text{-}6$$

The equation of motion of Lagrangian is identical for all coordinate systems, taking into consideration the interaction between the particles. Thus, the following function describes the properties of these interactions as well [20]:

$$L = \sum_{i=1}^{N} \frac{m\dot{r}^2}{2} - V(r_{1,\ldots\ldots,} r_N) \qquad 2\text{-}7$$

which can also be written in the Newtonian form as follows [20]:

$$m_i \ddot{r}_i = -\frac{dV(r_{1,\ldots\ldots,} r_N)}{dr_i} = F_i \qquad 2\text{-}8$$

This all means that potential energy is only dependent on the spatial configurations of the atoms, and that when they move, their potential energy changes as well.

g. Solving the Equation of Motion

In MD simulations, numerical schemes are used to solve the equations of motion and simulate the behaviour of a system of interacting particles over time. The primary goal is to obtain trajectories of the particles' positions and velocities as they evolve in time.

An integration algorithm to update the positions and velocities of particles at each time step must be used. The most commonly used algorithms in MD include the Verlet algorithm, velocity Verlet algorithm, and leapfrog integration.

- The Verlet algorithm is a simple and widely used method in MD. It updates the positions and velocities of particles based on their current positions, velocities, and forces. It is numerically stable and conserves energy in many cases.
- Velocity Verlet algorithm is similar to the Verlet algorithm, but also updates velocities in the middle of the time step, making it more accurate for some systems.
- Leapfrog integration is an algorithm that updates positions and velocities in a staggered manner, which is useful for conserving energy.

Only the Verlet algorithm will be explained in detail below.

The Verlet algorithm is particularly popular because of its simplicity and ability to accurately conserve energy over long simulation times. The Verlet algorithm updates particle positions and velocities based on their current positions, velocities, and forces.

Its fundamental concept involves crafting two third-order Taylor expansions for particle positions $r(t)$, one advancing in time and the other regressing. By denoting the velocities v as well as the accelerations a and the third derivatives of positions b with respect to time t as their respective counterparts, the following relationships emerge [20]:

$$r(t+\Delta t) = r(t) + v(t)\Delta t + \frac{1}{2}a(t)\Delta t^2 + \frac{1}{6}b(t)\Delta t^3 + \mathcal{O}(\Delta t^4) \qquad 2\text{-}9$$

$$r(t-\Delta t) = r(t) - v(t)\Delta t + \frac{1}{2}a(t)\Delta t^2 - \frac{1}{6}b(t)\Delta t^3 + \mathcal{O}(\Delta t^4) \qquad 2\text{-}10$$

Adding equations 2-9 and 2-10 gives:

$$r(t + \Delta t) = 2r(t) - r(t - \Delta t) + a(t)\Delta t^2 + \mathcal{O}(\Delta t^4) \qquad 2\text{-}11$$

This is the basic form of the Verlet algorithm.

h. Running the Simulation

To run an MD simulation, the initial dimensions and positions of all atoms, the potential function, and a time step must be defined. First, the simulation calculates the forces between the atoms, then using the equations of motions over the specific time step, the atoms are moved to a second position and the forces are calculated again. This sequence is repeated until the number of time steps required are done.

There are also some conditions that need to be specified, such as the ensemble average and the boundary conditions. There are two ensembles used, the NVE and the NVT, which ensure that the time and ensemble averages are equal. The NVE assumes that the number of atoms, the total volume and energy of the system is constant, which is not true in our case. Thus, the NVT ensemble is used, which assumes that the number of atoms, the total volume, and the temperature of the system is constant rather than the energy. Also, NPT ensembles are used to keep the number of atoms, total pressure of the system, and temperature constant.

i. Advantages and Limitations of MD Simulations

The major advantage of molecular dynamics simulations is that they are very effective in simulating the dynamics of physical and chemical processes at both microscopic and macroscopic scales. MD simulations can accurately predict the structure, dynamics, and interactions of atoms and molecules in a variety of conditions. Additionally, these simulations can calculate thermodynamic and kinetic properties, such as heats of formation, partition functions, and reaction rates.

On the other hand, the main limitation of MD simulations is that they are computationally intensive, requiring large amounts of computational power. Furthermore, because of the complexity of the systems being simulated, it is sometimes difficult to accurately determine force fields and parameters needed for the simulation. Additionally, MD simulations typically require a

large amount of time to reach equilibrium, and due to the complexity of the systems being simulated, some effects may not be accurately captured.

j. Non-equilibrium Molecular Dynamics (NEMD) Method

NEMD, otherwise known as the direct method, is used in Molecular Dynamics simulations to predict thermal conductivity. It is a useful tool, as it can offer insight into the heat transportation of partial systems instead of the thermal conductivity of the entire system – especially helpful for non-isotropic systems such as polymers [21]. To ensure steady heat flux, the temperature gradient and heat flux are often applied with the Langevin heat bath method, which is easier to employ than other methods like Muller's Plathe [22].

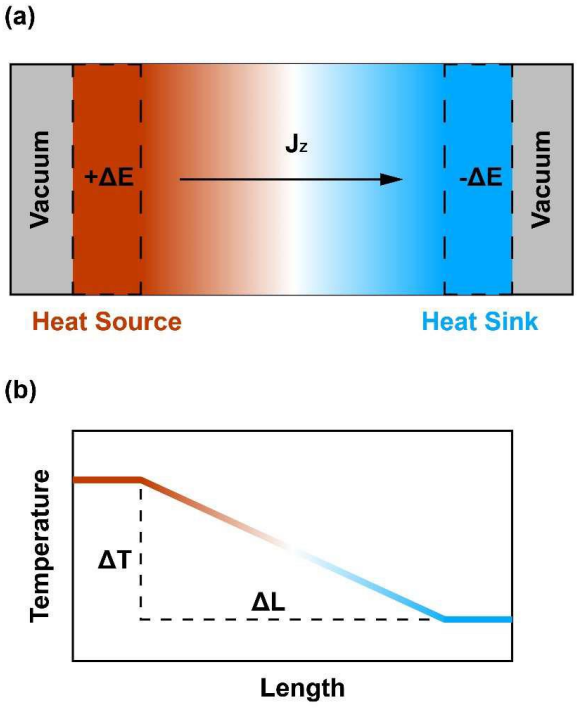

Figure 2-3 NEMD Model. (a) A periodic boundary condition model can be used to calculate the thermal transport of materials. It entails a red region as the heat source area, and blue region as the heat sink area. Vacuum is added at the two ends of the boundary to avoid horizontal heat transfer across the boundary. From the heat source, heat is only able to move to the heat sink, resulting in a heat current of Jz. (b) In the thermal transport simulation, a temperature distribution can be observed. ΔT is the temperature difference between the heat source and heat sink, while ΔL is the fitting length for thermal conductivity by Fourier's Law.

By rescaling particle velocities at each MD time step, the heat ΔE is added to a thin slab, while an equivalent amount is removed from another cantered slab of the same thickness. This will result in an increase or decrease of net kinetic energy, while potential energy remains unchanged. Eventually, when the system reaches a steady state, the heat current is given by $J_z = \frac{\Delta E}{\Delta t}$, where Δt is the period of the simulation, and Fourier's law is used to calculate the thermal conductivity.

The thermal conductivity relates the heat current to the temperature gradient via Fourier's law as [22]:

$$J_\mu = -\sum_v \lambda_{\mu v} \frac{\partial T}{\partial x_v} \qquad 2\text{-}12$$

where J_μ is a component of the thermal current, $\lambda_{\mu v}$ is an element of the thermal conductivity tensor, and $\frac{\partial T}{\partial x_v}$ is the gradient of the temperature T.

By running simulations with different systems sizes, the behaviours of an infinite system can be extrapolated. In, a schematic representation of the simulation cell is used to compute the thermal conductivity, with the presence of heat sources and sinks creating a current in the z-direction. However, this method only allows for the calculation of thermal conductivity in a single lattice direction. In contrast, the Green Kubo method does not suffer from this limitation and can calculate the entire thermal conductivity tensor in one simulation.

The direct method involves using high temperature gradients, which may not provide accurate results due to potential nonlinear effects that can occur outside the experimental range. To address this, it is important to test the effect of changing the thermal current on the calculated thermal conductivity. However, nonlinearity is acceptable with a specific set of temperature differences. In NEMD simulations, the boundaries of the heat source and sink can alter the atomic dynamics and limit the mean-free path, known as the Casimir limit. The mean-free path can be estimated by analysing smaller systems. NEMD is a commonly used method to calculate thermal conductance, as it directly shows the system's response to applied perturbations and is

efficient for large structures and perturbations. However, it has a larger size effect than the EMD method, as it can be impacted by scattering from the boundaries [23].

k. Equilibrium molecular dynamics (EMD) method

The Green-Kubo method is a technique for computing thermal conductivity using the EMD approach. This method involves linking the equilibrium current-current autocorrelation function to thermal conductivity through the Green-Kubo equation as follows [23]:

$$\lambda_{\mu v}(t_m) = \frac{1}{\Omega k_B T^2} \int_0^{tm} \langle J_\mu(t) J_v(0) \rangle \, d_t \qquad 2\text{-}13$$

where Ω is the volume, T is the temperature, k_B is the Boltzmann constant, and $\langle J_\mu(t) J_v(0) \rangle$ is the heat current autocorrelation function (HCACF).

At each molecular dynamics step, the heat current is calculated and saved. As the simulation proceeds in discrete MD steps with a step size of Δt, the calculation of heat current follows the equation above as a summation. The resulting equation, which is computed including the time averaging, is as follows [23]:

$$\lambda_{\mu v}(t_M) = \frac{1}{\Omega k_B T^2} \int_0^{tm} \sum_{m=1}^{M} (N-m)^{-1} \sum_{n=1}^{N-m} J_\mu(m+n) J_v(n) \qquad 2\text{-}14$$

where t_M is M Δt and $J_\mu(m+n)$ is the μth term of the heat current at time-step m+n.

It's important to remember that the number of integration steps (M) must be fewer than the total number of simulation steps (N). Typically, M is significantly smaller than N to ensure accurate statistical averaging. The bulk thermal conductivity, which is obtained in the limit M t → ∞, can be determined from the equation above as long as the integration time (Mt) is longer than the time required for current-current correlations to become negligible. Wang et al. suggest controlling the uncertainty of thermal conductivity predictions from the Green-Kubo method by

ensuring the ratio of integration time to total simulation time meets the convergence requirement [24].

Simulations are performed in equilibrium and transport coefficients are calculated using the Green-Kubo formula based on the fluctuation-dissipation theorem. This means there is no driving force, so the system is always in the linear-response regime. However, finite-size effects can impact the accuracy of the Green-Kubo method [25–26]. In addition, obtaining convergence in the current-current autocorrelation function may require very long simulation times [27].

EMD is used to determine the thermal conductivity and equilibrium state information of a system, considering discrete time-steps. Unlike NEMD, EMD doesn't involve any external perturbations. It provides the thermal conductivity in three dimensions in a single simulation, with a smaller size effect than NEMD, but at the cost of longer computation time.

l. Choosing the Appropriate Method

Schelling et al. provide a comprehensive review of atomic-level simulation methods for computing thermal conductivity and highlights the trade-offs and considerations involved in selecting the most appropriate method for a given problem [28]. It evaluates various atomic-level simulation methods for computing thermal conductivity and compares the strengths and weaknesses of each method, including their accuracy, efficiency, and computational resources required. It provides guidance for choosing the appropriate method for a given application, based on factors such as the size and complexity of the system, the desired level of accuracy, and the available computational resources.

The Non-Equilibrium Molecular Dynamics (NEMD) method is used according to Schelling et al. because it can overcome some of the limitations and challenges associated with other methods. The NEMD method involves applying a temperature gradient to a system and measuring the resulting heat flow, which allows for the direct calculation of thermal conductivity. This method can be more accurate and efficient than other methods, especially for systems with complex behaviour or nonlinear thermal transport properties like nanofluids. According to Schelling et al., NEMD can be more reliable for some systems, especially those with large temperature gradients or high thermal conductivity and can provide a more direct measurement of thermal conductivity.

However, NEMD can also be more computationally expensive and requires careful consideration of factors such as the size of the system and the desired level of accuracy.

In addition, Nejatolahi et al. [29] provide insights into the challenges and limitations of calculating the thermal conductivity of nanofluids using molecular dynamics simulations and highlight the importance of selecting the appropriate method based on the specific requirements of the system. In that study a comparison is made of Non-Equilibrium Molecular Dynamics (NEMD) and Equilibrium Molecular Dynamics (EMD) methods for calculating the thermal conductivity of nanofluids. Analysis of the accuracy and efficiency of NEMD and EMD methods, with a focus on their ability to accurately simulate the thermal conductivity of nanofluids in different regimes. The advantages and disadvantages of NEMD and EMD methods, including their computational cost, numerical stability, and applicability to different types of nanofluids, are discussed. The impact of various factors, such as fluid concentration, fluid type, and simulation conditions, on the accuracy and reliability of thermal conductivity calculations is examined. Nejatolahi et al. conclude by saying “We showed that, unlike the NEDM method, the traditional EMD method does not give physically acceptable results for the thermal conductivity of nanofluids”. This is in perfect agreement with Schelling et al. analysis.

2.2 Computer Simulations of Nanofluids

There have been numerous efforts to understand the thermal transport in nanofluids using simulation methods that can accurately depict the complex phenomena at the nanoscale. One such technique is Molecular Dynamics Simulation, which tracks the movement of solid and liquid atoms at a molecular level.

Different simulation techniques in MD simulations are described in table 2-1 like EMD, NEMD, and RNEMD.

Equilibrium Molecular Dynamics (EMD) is a computational simulation technique used to study the behaviour of molecules or atoms in a system at thermodynamic equilibrium. In EMD, the system is allowed to evolve over time under the influence of intermolecular forces, such as van der Waals and electrostatic interactions. Starting from an initial configuration, the positions and velocities of particles are tracked as they interact with each other. EMD simulations are valuable for understanding the properties of a system under specific thermodynamic conditions, like temperature and pressure, once equilibrium is achieved.

Non-Equilibrium Molecular Dynamics (NEMD) is a molecular simulation technique that deviates from equilibrium by applying external forces or gradients to a system. These perturbations drive the system away from thermodynamic equilibrium, allowing researchers to study transport properties and dynamic behaviour. For example, NEMD simulations can apply shear forces to study fluid flow or temperature gradients to investigate heat transport. By measuring the system's response to these perturbations, NEMD provides critical insights into transport coefficients like viscosity, thermal conductivity, and diffusion coefficients.

Reverse Non-Equilibrium Molecular Dynamics (RNEMD) is a specialized variant of NEMD used for calculating transport properties. In RNEMD, instead of applying an external perturbation to the system, simulations are run in reverse time after the system has achieved a non-equilibrium state. This unique approach involves time-reversal symmetry principles and carefully constructed algorithms to compute transport coefficients accurately. RNEMD is particularly useful in scenarios where applying an external perturbation is challenging or impractical.

showcases a list of molecular simulation studies on nanofluids, and some of the most noteworthy studies are discussed below.

Table 2-1: Molecular dynamics simulation studies of nanofluid using EMD & NEMD methods (where SS, LL, SL refer to the interaction of solid-solid, liquid-liquid, and solid-liquid particles respectively).

Reference	Potential Used	Method	Volume Concentration	Thermal Conductivity Enhancement
Nejatolahi et al. [29]	LJ for LL, SL, SS	NEMD	4.2%	1%
Nejatolahi et al. [29]	LJ for LL, SL, SS	EMD	4.2%	51.5%
Sarkar et al. [11]	LJ for LL, SL, SS	EMD	8%	52%
Li et al. [30]	LJ for LL, SL EAM for SS	EMD	0.5–2 vol%	10%
T. Khamliche et al. [31]	LJ for LL, SL EAM for SS	EMD	1%	15-24 % (Temperature dependant)
Lu Zhou et al. [32]	LJ for LL, SL EAM for SS	NEMD	1.28–5.12%	12.5-34.8%
J. Chen et al. [33]	LJ for LL, SL, SS	RNEMD	0.5-1.5%	4.77-12.95%
Achhal et al. [34]	LJ for LL, SL EAM for SS	EMD	0.19-7.66%	0.07-59%

Nejatolahi et al. [29] compares two MD simulation methods for calculating the thermal conductivity of nanofluids. The author used both NEMD and EMD to simulate thermal conductivity of nanofluids composed of copper (Cu) nanoparticles dispersed in argon, and compared the results. The first method, EMD, predicts a significant enhancement of the thermal conductivity of nanofluids, while the second method, NEMD, predicts almost no enhancement. An analysis is made to determine the minimum and maximum limits of the thermal conductivity of nanofluids and addresses the role of various mechanisms in enhancing thermal conductivity, such as Brownian motion and micro-convection. The study finally discusses the effects of

external forces on the centre of mass and linear momentum of the nanoparticles, and shows that they do not have a significant impact on the results. The authors conclude that NEMD simulations are more accurate than EMD simulations for calculating the thermal conductivity of nanofluids.

Sarkar et al. [11] used MD simulation and the Lennard-Jones potential to model the behaviour of a nanofluid system consisting of Argon and Copper. They used the Lennard-Jones potential for liquid atoms from Ar [17] and for solid atoms from Cu [35]. The solid-liquid interactions were determined using the Lorentz-Berthelot mixing rule. The thermal conductivity was calculated using Green-Kubo correlation. They found that thermal conductivity increased with increasing particle volume fraction, with a maximum enhancement of 52% at 8% volume fraction. They also observed two regimes of conductivity enhancement and found that the mean square displacement (MSD) of liquid atoms in the nanofluid was higher than liquid atoms in the base fluid. They concluded that the thermal enhancement was due to the enhanced motion of the liquid atoms caused by the presence of solid nanoparticles.

T. Khamliche et al. [29] investigates the thermal conductivity of Cu nanoparticle-based nanofluids using both experimental and molecular dynamics studies. The nanofluids were fabricated using a laser ablation process, and the thermal conductivity was measured using a transient hot-wire method. The molecular dynamics simulations were performed to study the behaviour of the nanofluids at the molecular level and to validate the experimental results. In the simulation, the nanofluid was modelled as a suspension of Cu nanoparticles in a liquid base fluid of ethylene glycol. The solid-liquid and liquid-liquid interatomic interactions were described using Lennard-Jones potential. For the solid-solid interactions, embedded atom model (EAM) potential was used. The thermal conductivity was calculated from the temperature gradient in the nanofluid by using the Green-Kubo method. In this method, the thermal conductivity was related to the autocorrelation function of the heat flux, which was obtained from the MD simulation. In the simulation, the size and concentration of the Cu nanoparticles were varied to study their effect on the thermal conductivity of the nanofluid. The simulations were carried out under isothermal conditions and were run for a sufficient amount of time to reach steady state. The results showed that the thermal conductivity of the nanofluids increased with increasing nanoparticle concentration. The enhancement in thermal conductivity was attributed to the enhanced heat transfer between the nanoparticles and the fluid, due to the presence of strong thermal bridges

between the nanoparticles and the fluid. The simulations showed that the nanoparticles in the nanofluids enhance the thermal conductivity by reducing the phonon mean free path and increasing the phonon-phonon scattering rate. Overall, the results of this study suggest that the laser fabrication of Cu nanoparticle-based nanofluids results in enhanced thermal conductivity compared to pure fluids. The combination of experimental and molecular dynamics studies provides a comprehensive understanding of the thermal behaviour of nanofluids, which can be useful for the design of efficient heat transfer systems. Overall, the results of this paper suggest that the laser fabrication method is effective in producing copper-based nanofluids with high thermal conductivity. The molecular dynamics simulations confirmed the experimental results and provided additional insights into the thermal transport mechanisms in the nanofluids.

Lu Zhou et al. [32] investigated the effect of nanoparticle aggregation on thermal conductivity enhancement in nanofluids. NEMD was used to analyse the thermal conductivity of nanofluids containing nanoparticles with different aggregation levels. The nanofluids were modelled as suspensions of copper nanoparticles in an argon base fluid. The solid-liquid, liquid-liquid, and solid-solid interatomic interactions were described using the Lennard-Jones potential. The simulations were designed to study the effect of nanoparticle size, concentration, and aggregation on the thermal conductivity of the nanofluids. To investigate the effect of nanoparticle aggregation, the simulations were performed for both isolated nanoparticles and nanoparticles that were allowed to aggregate. The simulation results were compared with experimental data to validate the accuracy of the simulations, and to identify the key factors that contribute to thermal conductivity enhancement in nanofluids. The results showed that nanoparticle aggregation can enhance the thermal conductivity of nanofluids due to the increased thermal transport caused by the higher surface area-to-volume ratio of the aggregates. The study found that the thermal conductivity of nanofluids increased significantly when the nanoparticles aggregated to form large clusters, and the thermal conductivity increased with the increase in the size of the clusters. However, the increase in thermal conductivity was found to be limited by the formation of stable nanoparticle clusters. The study also showed that the size of the nanoparticles and the type of base fluid had a significant impact on the thermal conductivity of the nanofluids. Based on these findings, the author concludes that nanoparticle aggregation plays a crucial role in the thermal conductivity enhancement of nanofluids, and that the structure of the aggregates and the size of the nanoparticles have a significant impact on the thermal conductivity of the nanofluids. The

importance of considering both the size and the concentration of nanoparticles in the design of nanofluids for thermal management applications is also highlighted.

J. Chen et al. [33] used reverse non-equilibrium molecular dynamics (RNEMD) simulations to investigate the enhanced thermal properties of CuAr nanofluids. The main difference between RNEMD and NEMD lies in the direction of heat flow. In NEMD, the heat flow direction is from a high temperature region to a low temperature region, whereas in RNEMD, the heat flow direction is from the low temperature region to the high temperature region. The solid-liquid, liquid-liquid, and solid-solid interatomic interactions were described using the Lennard-Jones potential. The simulations were performed on nanofluids with different volume fractions of copper particles. The simulation process involves introducing thermal heat flux from one end of the nanofluid system to the other, with the temperature gradient driving the molecular motion in the nanofluid. The temperature profile, heat current, and thermal conductivity of the nanofluids are then analysed. The results showed that the thermal conductivity of nanofluids increases as the volume fraction of nanoparticles increases, and non-linearly decreases with the increase of the particle size. The concentration of nanoparticles in the nanofluid affects the energy transfer process and has a significant impact on the fluid's temperature gradient when the particle size is small. The improvement of the thermal conductivity of nanofluids is also linked to the adsorption of nanoparticles by the liquid molecules. As the concentration of nanoparticles increases, the particles within the nanofluid become more closely associated and interact more with each other. However, as the particle size increases, the aggregation and interaction between the particles decreases. The solid-liquid interaction causes the nanoparticles to adsorb liquid molecules more readily, leading to the nanofluid having a crystal-like microstructure.

Achhal et al. [34] carried out simulations to study the effect of particle size and temperature on the thermal conductivity of nanofluids. The study was done using EMD, for a nanofluid system of copper and argon. The solid-liquid and liquid-liquid interatomic interactions were described using Lennard-Jones potential and solid-solid interactions using Embedded Atom Model (EAM) potential that takes the metallic bonding into account. The results showed that the relative thermal conductivity enhancement of the nanofluid increased as the volume fraction increased from 0.19% to 7.66% due to the decrease of fluid condensation around the nanoparticles. Additionally, it was found that thermal conductivity and relative thermal conductivity both increased with temperature in the range of 86 K to 102 K, with a more significant effect observed at high particle

concentrations. The study highlights the importance of particle size and temperature in improving the efficiency of nanofluids.

As discussed, several studies have been conducted to understand the thermal conductivity behaviour of nanofluids, with different methodologies and simulation approaches being used. The general consensus was that the thermal conductivity of nanofluids can be enhanced by the presence of nanoparticles, with the extent of enhancement depending on various factors such as nanoparticle size, concentration, and aggregation. The use of molecular dynamics simulations was found to be useful in understanding the thermal behaviour of nanofluids, and the combination of experimental and simulation results provided a comprehensive understanding of thermal transport mechanisms in nanofluids. These results can be useful for the design of efficient heat transfer systems using nanofluids.

2.3 Thermal Conductivity Enhancement Mechanisms in Nanofluids

Different studies [36–38] have discussed various thermal conductivity enhancement mechanisms in nanofluids, including Brownian motion of nanoparticles, clustering of nanoparticles, nanolayering of the liquid at the liquid/nanoparticle interface, ballistic transport and nonlocal effect, thermophoretic effect, and near-field radiation. Many models have been developed to explain these mechanisms or a combination of them, and they have been successful in fitting experimental data. However, the fact that different models based on different mechanisms can explain the same or similar data does not provide a deeper understanding of the mechanisms. A closer examination uncovers that the fitting parameters are often not physically accurate.

a. Brownian Motion

In various studies [37], [39], [40], there have been differing opinions regarding the significance of Brownian motion in enhancing thermal conductivity. Einstein laid the foundation for the theory of Brownian motion and derived the basic relationship between the diffusivity a of a particle in a fluid with viscosity μ [41]:

$$a = \frac{k_B T}{3\pi d\mu} \qquad 2\text{-}15$$

where "d" is the diameter of the particle, and "k_B" the Boltzmann constant.

The conventional theory for Brownian motion often begins with the Langevin equation, which governs the instantaneous velocity of the Brownian particle and can be expressed as [44]:

$$m\frac{dv}{dt} = -m\eta v + R(t) \qquad 2\text{-}16$$

where "m" represents the Brownian particle, "R(t)" is the random driving force, and "η"is the friction coefficient. For a spherical Brownian particle in a fluid, the Stokes law determines that η = 3πdμ/m. Solving the Langevin equation shows that the velocity of the Brownian particle decreases exponentially with a time constant [44]:

$$\tau = \frac{1}{\eta} = \frac{m}{3\pi d\mu} = \frac{\rho d^2}{18\mu} \qquad 2\text{-}17$$

The average speed of the Brownian particle is expressed as [44]:

$$v = \sqrt{\frac{3k_B T}{m}} \qquad 2\text{-}18$$

Typically, the thermal conductivity of bulk crystalline solids decreases with temperatures at or above room temperature. Phonons in crystalline solids have a diverse range of mean free paths. Based on the kinetic theory, the thermal conductivity can be represented as [48]:

$$k = \frac{1}{3}\int C(\omega)\, V(\omega)\, \Lambda(\omega)\, d\omega = \frac{1}{3} CV\Lambda \qquad 2\text{-}19$$

were "C" being the specific heat per unit volume, "V" the phonon group velocity, and "Λ" the mean free path.

By utilising the above relations, it is possible to quickly calculate the maximum contribution from Brownian motion. Based on the kinetic expression in the equation above, despite its limitations for liquid environments, the thermal conductivity contribution from Brownian particles is proportional to [48]:

$$k_{\text{Brownian}} = \frac{1}{3} CV\Lambda = \frac{1}{3} CV^2\tau = \frac{k_B TC}{3\pi d\mu} \qquad 2\text{-}20$$

Using the same reasoning, the above expression can also be applied to the liquid itself, and the ratio of the Brownian particles' contribution to the thermal conductivity to that of the base fluid is [48]:

$$\frac{k_{\text{Brownian}}}{k_{bf}} = \frac{(C/d)_{np}}{(C/d)_{bf}} \qquad 2\text{-}21$$

where bf and np stand for base fluid and nanoparticles, respectively.

The thermal conductivity contribution from Brownian motion is likely to be two orders of magnitude smaller than that of the base fluid, as the molecular diameter of the base fluid is

usually much smaller than that of the nanoparticle. This is true even if the specific heat per unit volume of the nanoparticles is assumed to be equal to that of the base fluid, since the Brownian motion of the nanoparticles causes the surrounding fluid molecules to move at a similar pace. If only the specific heat of the nanoparticles is considered, the thermal conductivity ratio will be further reduced by the volume fraction of the nanoparticles. Therefore, models that are based purely on the motion of the nanoparticles are questionable. This was pointed out early in the debate on the role of Brownian motion by Keblinski and Cahill [42].

An argument in favour of the significance of Brownian motion is the microconvection argument. Expressions for convective heat transfer coefficients between a heated sphere and a cold surrounding fluid have been used to explain thermal conductivity enhancement in nanofluids, with a good fit to experimental data [39], [43]. This is based on the assumption that the velocity of the surrounding fluid is equal to the average thermal velocity of the Brownian particles. However, these models lack a clear physical explanation connecting heat conduction through liquids and nanoparticles to heat transfer from a nanoparticle maintained at a constant temperature.

In models that only consider the kinetic motion of nanoparticles, the potential interactions between the particles were not taken into account. Bhattacharya et al. [44] studied the potential interactions by using the Langevin equation and the Green—Kubo formulation. However, the parameters used in their potential function were found to be too strong compared to real nanofluids. In another study, the electrothermal effect, which involves the long-range energy exchange between nanoparticles through the electrical double layer and their random Brownian motion, was considered [45]. Although the theoretical treatment was sound, an error in numerical substitution led to the incorrect conclusion that the electrothermal effect was significant. Numerical calculations showed that the effect was too weak to explain the experimental observations. As a result, it was concluded that the potential interactions between the Brownian motion of nanoparticles are not enough to explain the experimental data.

One key aspect of the Brownian motion picture that has yet to be fully understood involves the steady state assumption made in the Langevin equation. This equation assumes that the nanoparticle is in a constant state of motion, and the drag on it remains the same. However, including the transient effect of the Stokes flow would result in a memory effect and an integral

Langevin equation. The solution of this equation shows that the velocity decay follows a power law instead of an exponential function, as originally discovered through computational simulation [46]. This power law decay is much slower than the exponential decay, and this has been used as a basis for developing a kinetic argument by Xuan et al. [47] and Yang [48]. However, a rigorous solution of the retarded Langevin equation has shown that the Einstein relation, which was obtained under the assumption of exponential decay, still holds true, casting doubt on the power-law based kinetic picture. Additionally, molecular dynamics simulations have indicated that the hydrodynamic effect caused by Brownian motion is not enough to explain the increased thermal conductivity [49–50].

b. Clustering

Although the simplest explanation for nanofluids is that nanoparticles are isolated and evenly dispersed in the liquid, the reality of suspensions of nanoparticles in liquids is more complex. Nanoparticles can interact, group together, and form internal structures [51–53]. Studying these structures falls under the field of soft materials, a large branch of condensed matter physics. These internal structures of nanofluids may be able to explain experimental results. The idea that nanoparticles form clusters and that these clusters can explain experimental results, has been mentioned in several studies [54–57]. Prasher et al. [54] started with the notion that clusters of nanoparticles, which have a larger effective volume, along with their Brownian motion, can account for the experimental data, and then moved on to develop a three-level homogenisation model based on effective media theory without considering Brownian motion, and suggested that these models can explain experimental observations.

c. Liquid Layering

The structure of liquids near solid surfaces can be impacted by the potential of the solid, leading to the formation of crystalline layers, usually 1 to 5 atomic layers thick [58]. This is sometimes suggested as a reason for the increased thermal conductivity in nanofluids. However, as noted by Xue et al. [59], the liquid layering is unlikely to be the explanation for the experimental observations. In addition, the reduced thermal conductivity of 1 to 5 atomic layer crystal films due to phonon size effects in solids further weakens the possibility that liquid layering is the cause of increased thermal conductivity.

d. Ballistic Transport and Nonlocal Effects

Ballistic transport occurs when internal scattering mechanisms are insufficient, leading to a dominance of boundary and interfacial scattering [60]. This results in nonlocal heat conduction. Reduced thermal conductivity in solid nanostructures is one example of ballistic transport, while nonlocal transport outside a nanostructure occurs when the heat carrier mean free path in the surrounding medium is much greater than the length of the nanostructure itself [61–62]. Both ballistic and nonlocal transport processes are expected to result in lower heat transfer than predicted by diffusion theory based on bulk material properties. Thus, it is unlikely that these processes are responsible for the observed enhanced thermal conductivity in nanofluids. Kumar et al. [63] proposed a kinetic theory model that considers ballistic transport of nanoparticles in the liquid, but this would require the solid nanoparticles' mean free path in the liquid to be in the centimetre range, which is unrealistic [42].

e. Thermophoresis

Thermophoresis refers to the movement of nanoparticles caused by a temperature gradient. When the temperature is higher on one side, the particles on that side experience greater force from the energetic molecules, causing them to move to the cooler side. This could impact the thermal conductivity measurements [64]. However, when the hot-wire temperature was altered in the experiment, leading to a change in the temperature gradient, no significant change was observed in the measured thermal conductivity. This indicates that thermophoresis is not a significant factor. An analysis by Koo and Kleinstreuer also concluded that thermophoresis does not contribute significantly to thermal conductivity enhancements [65].

f. Near-field radiation

Domingues et al. [66] conducted molecular dynamics simulations that showed that heat transfer between two nanoparticles increases rapidly as they get closer. This led to the suggestion that near-field radiation may be responsible for the increased thermal conductivity. While experiments have shown that near-field radiation can be much higher than the maximum radiation exchange described by blackbodies [67], it is still much smaller than heat conduction

through a medium. When two surfaces are in close proximity, the distinction between radiation and conduction becomes less clear. If the surfaces are in complete contact, the thermal boundary resistance between them would apply. Therefore, it is unlikely that near-field radiation is the cause of the observed increased thermal conductivity.

2.4 Parameters That Govern Thermal Conductivity Enhancement in Nanofluids

It is evident that the thermal conductivity of a nanofluid is influenced by various factors, such as the base fluid material, nanoparticle material, the shape and size of the nanoparticles, the use of surfactants, and the pH of the nanofluid, among others [68].

a. Type of Carrier Fluid Used

It was discovered that the thermal conductivity of the synthesised fluid is largely influenced by the thermal conductivity of the base fluid used. In a study by Barbes et al. [69], CuO nanoparticles of average size 25 nm were dispersed in a water-ethylene glycol base fluid. Results showed that, regardless of the volume fraction and temperature of the nanofluid, the thermal conductivity of water-CuO nanofluid was higher compared to that of ethylene glycol-CuO nanofluid.

Agarwal et al. [70] investigated the thermal conductivity of different nanofluids by dispersing CuO nanoparticles with an average size of 45 nm in various carrier fluids, including distilled water, ethylene glycol, and engine oil. They found that the thermal conductivity of the distilled water-based nanofluid was the highest due to the higher thermal conductivity of distilled water compared to the other two base fluids.

b. Type of Nanoparticles Used

It was found that the type of nanomaterial has a significant impact on the thermal conductivity of the nanofluid, but the thermal conductivity of the nanomaterial alone is not the sole determining

factor. The size and clustering of particles also play a crucial role in the thermal conductivity of the nanofluid [71–75]. This was demonstrated in a study by Yoo et al. [76] who synthesised nanofluids using TiO2 and Al2O3 nanoparticles in water. Although Al2O3 nanoparticles have higher thermal conductivity than TiO2 nanoparticles, the nanofluid made with TiO2 showed higher thermal conductivity. This was attributed to the smaller average particle size (25 nm) of the TiO2 nanoparticles compared to the Al2O3 nanoparticles (48 nm). The researchers concluded that the thermal conductivity of the nanoparticles is not the main factor that determines the thermal conductivity of the nanofluid; rather, the surface area-to-volume ratio of the particles plays a key role. Another study by Pang et al. [77] measured the thermal conductivity of Al2O3-methanol and SiO2-methanol nanofluids and found that the former had higher thermal conductivity due to higher aggregation of SiO2 nanoparticles.

c. Nanoparticle size

Researchers found that the higher the surface area to volume ratio of nanoparticles, the higher the thermal conductivity of the nanofluid. This can be achieved by using smaller particles [78]. Wang et al. [79] studied the effect of particle diameter and volume fraction on thermal conductivity using Al2O3 and CuO nanoparticles in deionised water, engine oil, and ethylene glycol. Results showed that thermal conductivity increased as particle size decreased at a given volume fraction of nanoparticles. Patel et al. [80] investigated the effect of particle size on thermal conductivity of Al2O3 nanofluid in water and ethylene glycol and concluded that thermal conductivity is inversely proportional to particle size. The authors attribute this to a higher surface-to-volume ratio, higher particle velocity, and more rapid Brownian motion caused by smaller particles.

d. Nanoparticle Shape

The surface area to volume ratio of nanoparticles has a significant impact on thermal conductivity of nanofluid, and this ratio is also affected by the shape of the nanoparticles. Maheshwary et al. [81] found that the maximum thermal conductivity was seen in cubical TiO2 nanoparticles (52 nm in size), followed by cylindrical (40 nm to 53 nm), and spherical (25 nm) particles. Despite their lower thermal conductivity, spherical particles are widely used in heat transfer applications because of their lower cost, higher stability, and better tribological properties. On the other hand,

cubical particles are less popular due to their higher cost, despite their better thermal conductivity performance. Murshed et al. [82] investigated the effect of TiO2 nanoparticle shape on thermal conductivity and found that rod-shaped particles had higher thermal conductivity compared to spherical particles for all volume fractions.

e. Temperature of Nanofluid

Many studies have been conducted to understand the effect of temperature on the thermal conductivity of nanofluid, with results indicating an increase in thermal conductivity with rising fluid temperature. The variation in thermal conductivity with temperature can be attributed to the influence of Brownian diffusion and thermomigration on the temperature of the nanofluid. Sundar et al. [83] found that the thermal conductivity of Fe3O4 water and ethylene glycol nanofluid increased with temperature. Kole and Day [84] investigated the thermal conductivity of CuO lubricating oil nanofluid at various temperatures and found that thermal conductivity increased by 10% and 12% at 30°C and 80°C, respectively, for a 2.5% volume fraction.

2.5 Impact of Enhanced Thermal Conductivity on BTMS

Thermal conductivity enhancement can lead to significant improvements in the performance, efficiency, and reliability of BTMS [85].

Thermal conductivity in nanofluids can efficiently dissipate heat generated during battery operation. This efficient heat removal is crucial in preventing the battery from reaching excessive temperatures, ensuring it operates within a safe and optimal thermal range. This is particularly crucial in high-energy-density batteries, such as those used in electric vehicles, which can generate significant heat during charging and discharging.

Batteries operating at elevated temperatures can experience reduced efficiency, accelerated degradation, and even safety risks. With improved thermal conductivity, it becomes easier to maintain optimal operating temperatures, thereby extending battery life and ensuring safer operation. Batteries operating at higher temperatures are less efficient. By maintaining lower

operating temperatures through improved thermal management, the overall energy efficiency of the battery system can be enhanced.

Hotspots, localized areas of elevated temperature, can develop within battery packs, leading to thermal stress and potential safety hazards. Enhancing thermal conductivity helps distribute heat more evenly throughout the battery, reducing the risk of hotspots and associated problems.

Higher thermal conductivity enables batteries to operate at higher power densities, which is essential for applications requiring rapid energy discharge or charging. Electric vehicles, for example, could benefit from improved acceleration and regenerative braking capabilities.

In BTMS, cooling components such as fans or liquid cooling systems can add weight, complexity, and energy consumption. Improved thermal conductivity can reduce the reliance on these cooling mechanisms, leading to more energy-efficient and lightweight designs.

Fast charging is desirable in electric vehicles and consumer electronics. Improved thermal conductivity can enable faster charging by dissipating the heat generated during rapid charging more effectively, thereby reducing the risk of overheating.

Longer battery lifespans and reduced cooling requirements can translate into cost savings for manufacturers and end-users. Batteries that last longer and require less maintenance are more economically attractive.

3. Methodology

In this section, a comprehensive overview of the methodology employed in this study to determine the thermal conductivity of a nanofluid system through Non-Equilibrium Molecular Dynamics (NEMD) simulations is provided. The primary focus of this study is modelling a nanofluid system composed of copper and silver nanoparticles dispersed within a base fluid, polyalphaolefin (PAO-2) at different volume fractions.

3.1Software

List of all the software used in this work is mentioned in this section.

a. LAMMPS

All simulations in this study were preformed using LAMMPS.

LAMMPS, which stands for Large-scale Atomic/Molecular Massively Parallel Simulator, is a molecular dynamics program that was developed by Sandia National Laboratories [86]. This software is free and open source, distributed under the GNU General Public License, and was first released in 1995. LAMMPS uses the Message Passing Interface for parallel communication and is available for various operating systems including Linux, OS X, and Windows. The original code was written in C++ and was developed under a joint agreement between two laboratories from the US Department of Energy and three private sector firms.

LAMMPS is known for its efficient computation, and it achieves this through its use of neighbour lists (Varlet lists) to track neighbouring atoms. The simulation can be optimized for each system by adjusting the neighbour list. For parallel computing, LAMMPS uses spatial-decomposition techniques where the simulation domain is divided into partitions, with each processor responsible for a specific subdomain. These processors communicate with each other and store information about atoms that are located on the boundary of their subdomains [86], [87]. LAMMPS has made significant contributions in fields such as heat transfer, fluid mechanics, composite materials, biological science, and more.

b. Moltemplate

Moltemplate is a general and flexible tool for creating molecular dynamic (MD) simulation input files [88]. It is used to define molecular systems using a simple and intuitive text-based format. Moltemplate automatically generates valid simulation input files for various MD simulation engines (such as LAMMPS) from these definitions. It supports a wide range of inter-particle potentials and provides a variety of built-in options for defining bond, angle, dihedral, and improper interactions. This allows users to define complex molecular systems efficiently and effectively, which can be useful in various applications such as studying the properties of materials, predicting reaction kinetics, and modelling biological systems. Moltemplate is written in Python and is freely available under an open-source license.

Moltemplate was used in this study to prepare the input data file for the PAO-2 simulations.

c. OVITO

OVITO, or Open Visualization Tool, is a free software for visualizing and analysing atomistic data from large-scale molecular dynamics and Monte-Carlo simulations [89]. Its aim is to provide flexibility and reliability in visualization. These simulations are widely used to model materials at an atomic level and generate 3D atomic configurations and the movement of atoms. To effectively analyse and understand these complex systems, a powerful visualization tool is crucial. OVITO serves this purpose by converting raw data into an understandable atomic representation, allowing for deeper insights into the simulation. OVITO is written in C++ and can run on Microsoft Windows, MacOS, and Linux. Some of its key features include coordination number analysis, radial distribution function, displacement vector calculation, atomic strain tensors, and histogram, scatter plot, and bin-and-reduce functions.

All simulations were visualised by OVITO.

d. Visual Molecular Dynamics (VMD)

Visual Molecular Dynamics (VMD) is an open-source molecular visualization and analysis software primarily designed for researchers in the fields of chemistry, biology, and biophysics. Developed by the Theoretical and Computational Biophysics Group at the University of Illinois

at Urbana-Champaign [90], VMD is a powerful tool that enables scientists to visualize, analyse, and manipulate large biomolecular systems, such as proteins, nucleic acids, and lipid bilayers.

VMD provides a wide range of features, including:

- VMD can read and write a wide variety of molecular file formats, including PDB, CHARMM, AMBER, GROMACS, and NAMD, among others.
- VMD is equipped with advanced algorithms and rendering techniques that enable real-time visualization of large molecular systems, even on modest hardware.
- VMD offers a comprehensive set of built-in analysis tools, such as distance measurements, angle calculations, hydrogen bond identification, secondary structure analysis, and more.
- Users can tailor the VMD interface to their specific needs and preferences, thanks to a robust scripting language that allows for the creation of custom scripts and plugins.
- TopoTools is a plugin for the VMD software that provides utilities for the creation, manipulation, and analysis of topological information in molecular systems. Developed by Axel Kohlmeyer [91], TopoTools is particularly useful for preparing and processing input and output data for molecular dynamics simulations using LAMMPS.
- VMD runs on various operating systems, including Windows, macOS, and Linux, and can be used on a wide range of hardware, from desktops to high-performance computing clusters.

All pictures of the simulations shown in this thesis were obtained using VMD.

3.2 General Methodology Used in this Study

NEMD simulations were carried out to determine the thermal conductivity of a Nanofluid system. Nanofluid systems were modelled by suspending copper and silver nanoparticles of different volume fractions in base fluid PAO-2.

Using PAO-2 as a base fluid was not based on scientific reasoning. The choice was made due to the availability of information about PAO-2 in the research group and its use in other projects.

In this study, the properties of polyalphaolefin (PAO-2), a commonly used synthetic oil is simulated. With a kinematic viscosity of 2 cSt or 2 mm2 s^{-1} at 373 K, PAO-2 is a popular choice

as the base fluid for lubricants due to its high viscosity index, low-temperature fluidity, and high oxidative and chemical stability [92]. Additionally, its biodegradable properties [93] and safe usage make PAO-2 a suitable option for use as a coolant in various electromechanical devices.

The PAO-2 base fluid is represented by 9,10-dimethyloctadecane (C20H42), which is commonly found in PAO-2 oil [94]. To simulate the base fluid, a simulation box containing molecules of 9,10-dimethyloctadecane [95] was created.

System setup:

The system was modelled using a cubic simulation box of size 50 x 50 x 100 Å filled with copper atoms and PAO-2 molecules. The initial configuration was generated using a random placement of atoms with a specified number density. This have been achieved using the Moltemplate software [88]. The time-step used in this study is 0.04 fs.

Force field:

In this simulation, the L-OPLS-AA force-field [44–45] is utilized to model the PAO-2 interactions, which has a generic form as follows [97]:

$$V(r) = \sum_{bonds} k_b(b - b_0)^2 + \sum_{angles} k_\theta(\theta - \theta_0)^2 + \sum_{dihedrals} \sum_{n=1}^{4} k_\emptyset(1 + (-1)^{n-1}\cos(\emptyset)) + \sum_{vdW} 4\epsilon_{ij}\left[\left(\frac{\sigma}{r_{ij}}\right)^{12} - \left(\frac{\sigma}{r_{ij}}\right)^{6}\right] + \sum_{coulomb} \frac{q_i q_j}{\epsilon_0 r_{ij}} \quad (3\text{-}1)$$

where the right-hand side of the equation computes the bonded interaction energies from bond stretching, bending, and torsions. The van der Waals and electrostatic interactions are calculated by the last two terms. The bonding energies, Lennard-Jones parameters for modelling van der Waals energies, and partial charges for electrostatics used are listed in the tables below [96–99].

Table 3-1 Bonding parameters used in term 1 in equation v(r).

Bond	k_b (kcal mol^{-1}Å^{-2})	b_0 (Å)
C-C	268	1.529
C-H	340	1.090

Table 3-2 Angle parameters used in term 2 in equation v(r).

Angle	k_θ(kcal mol^{-1} rad^{-2})	θ_0(deg)
C-C-H	37.50	110.7
H-C-H	33.00	107.8
C-C-C	58.35	112.7

Table 3-3 Dihedral parameters used in term 3 in equation v(r).

Dihedral	$k_{\emptyset 1}$ (kcal mol^{-1})	$k_{\emptyset 2}$ (kcal mol^{-1})	$k_{\emptyset 3}$ (kcal mol^{-1})	$k_{\emptyset 4}$ (kcal mol^{-1})
C-C-C-C	0.6446926386	-0.2143420172	0.1782194073	0.0000
H-C-C-H	0.0000	0.0000	0.3000	0.0000
C-C-C-H	0.0000	0.0000	0.3000	0.0000
C-C_{CH}-C-C	1.3000	-0.0500	0.2000	0.0000
C_{CH}-C-C-C	1.3000	-0.0500	0.2000	0.0000
C-C_{CH}-C_{CH}-C	1.3000	-0.0500	0.2000	0.0000
C_{CH}-C_{CH}-C -C	1.3000	-0.0500	0.2000	0.0000

Table 3-4 LJ parameters & partial charges of the atoms used in terms 4 and 5 in equation v(r).

Atom type	k_{ij} (kcal/mol)	σ_{ij} (Å)	$q_i(e^-)$
C_{CH3}	0.066	3.5	-0.222
C_{CH2}	0.066	3.5	-0.148
C_{CH}	0.066	3.5	-0.060
H_{CH3}	0.030	2.5	0.074
H_{CH2}	0.026	2.5	0.074
H_{CH}	0.030	2.5	0.060

Minimization:

Minimization in molecular dynamics refers to the process of finding the minimum energy configuration of a system of interacting particles. This process is used to remove any initial

positional or thermal fluctuations in the system and bring the particle coordinates to a configuration that corresponds to the minimum potential energy. The minimization is achieved by iteratively adjusting the particle positions so as to minimize the potential energy of the system. This is typically done using a gradient-based optimization method, such as conjugate gradient or steepest descent, in which the particle positions are updated in the direction of the negative gradient of the potential energy. The minimization process is typically performed prior to performing the actual molecular dynamics simulation, in order to ensure that the system is in a physically meaningful configuration before the dynamics are computed.

The Polak-Ribiere version of the conjugate gradient algorithm, referred to as "cg", is utilized in this study. The algorithm computes the force gradient at each iteration and combines it with previous iteration information to determine a new search direction, which is conjugate to the previous direction. The PR variant of the CG method is known to be the most effective choice for many problems, as it adjusts the direction choice and restarts the CG method when progress ceases.

The stopping tolerance for energy used is $1x10^{-13}$ (unitless) and stopping tolerance for force used is $1x10^{-12}$ (kcal/mol)/Angstrom. In addition, the maximum iterations of the minimizer were chosen to be 1000 and the maximum number of force/energy evaluations was 10000.

Equilibration:

The system was equilibrated first for 40 picoseconds at temperatures ranging 293, 313, 333, 353, and 373 K, where separate runs were performed for each temperature separately. This equilibration was preformed using an NPT ensemble.

The second equilibration step was performed for 40 picoseconds also at temperatures ranging 293, 313, 333, 353 , and 373 K, where separate runs were performed for each temperature separately. This equilibration was preformed using an NVT ensemble.

This equilibration was performed to remove any residual forces from the initial configuration and to reach a steady state.

The third and final equilibration step was performed to apply the heat flux under an NVE ensemble. This equilibration took 80 picoseconds. The heat added and subtracted from the two regions is 0.0001 kcal/mol.

Production Run:

After equilibration, the production run was performed for 160 picoseconds. The temperature of the system was kept constant via an NVE ensemble, and the heat flux was calculated.

In the discussed MD simulations, random initial velocities and temperatures was used as a means to ensure the statistical representativeness of their findings while averting the introduction of potential biases. It is important to note that this common practice in MD simulations was complemented by the implementation of a seeding number or random number generator (RNG) to govern the stochasticity of the initial conditions.

More specifically, a meticulously defined seed value was adopted for the RNG. This particular seed value played a pivotal role in establishing uniformity in the generation of random numbers at the commencement of each simulation run. This uniformity, engendered by the constant seed, bore significance for three primary objectives:

Firstly, the utilization of a fixed seed value guaranteed the reproducibility of the simulations. This was of paramount importance, as it allowed for the precise replication of simulation conditions—a fundamental aspect for results validation and the facilitation of additional runs and subsequent analyses.

Secondly, in scenarios necessitating multiple simulation runs for the purpose of ensemble averaging or the attainment of statistically robust outcomes, the steadfast use of a fixed seed ensured that the randomness introduced across individual runs remained consistent. This congruity formed the bedrock for confident ensemble averaging and various other essential statistical procedures.

Lastly, the employment of a fixed seed acted as a proactive measure to avert the introduction of systematic bias. By mitigating the impact of variability stemming from initial condition disparities, the researchers effectively minimized the potential for inadvertent prejudicial influences.

It should be noted that the definition of simulation parameters in MD simulations, such as the time step and the size of the simulation box, involves a combination of scientific judgment, computational considerations, and physical principles. The choice of the time step often depends

on the physical properties of the system being simulated. It should be small enough to accurately capture the fastest motions in the system. The Nyquist theorem suggests that the time step should be smaller than half of the fastest oscillation or vibration period of interest. A critical factor in choosing the time step is numerical stability. A time step that is too large can lead to numerical instability in the simulation. Stability criteria depend on the integration algorithm used (e.g., Verlet, leapfrog) and the force field parameters. Initial time step values are often chosen based on experience and prior knowledge, and then the simulation is run and monitored for stability. If instability is observed, the time step is reduced until stability is achieved.

3.3 Calculating Thermal Conductivity

The fix eHEX command in LAMMPS can be used to calculate thermal conductivity using the NEMD direct method. The NEMD direct method is a non-equilibrium method that involves applying a heat flux to a system and measuring the resulting temperature gradient. The thermal conductivity can then be calculated from the heat flux and temperature gradient using the Fourier law of heat conduction.

To use fix eHEX to calculate thermal conductivity in the direct method NEMD, two regions are created in the simulation box: a hot region and a cold region, where energy is being added and subtracted respectively. eHEX fix is an implementation of the asymmetric version of the enhanced heat exchange algorithm developed by Wirnsberger [100]. The eHEX algorithm extends the heat exchange algorithm developed by Ikeshoji [101] by incorporating additional coordinate integration to account for higher-order truncation terms in the operator splitting. In this method, heat is transferred by rescaling velocities appropriately, adding a certain amount of heat to one region and removing it from another. Fix eHEX was chosen because of the excellent energy conservation of this method.

To add or subtract energy, the velocities of atoms in the heat source or heat sink regions are rescaled. The thermal conductivity of a system can be determined using Fourier's law of conduction, which states that [100]:

$$k_{zz} = -\frac{J_z^q}{\partial T / \partial Z} \qquad 3\text{-}2$$

where

$$J_z^q = \frac{\dot{Q}}{2L_xL_y} \qquad 3\text{-}3$$

Lx and Ly are the lengths of the simulation box in the x and y directions. The value of $\partial T/\partial Z$ is obtained by averaging the slopes of the linear profiles on the left and right sides. Q (kcal/mol) is the energy added and subtract from the 2 regions. The factor of 2 in the denominator is due to the periodic boundary conditions, which result in half of the added energy to the heat source flowing to the left. Temperature profile data is collected during the final 40000000 k timesteps.

4. Results & Discussions

4.1Validation

To ensure accuracy and validity of the used model, the methodology and interatomic potentials employed in this research was validated by comparing the thermal conductivity of the base fluid (liquid argon) with both experimental data and other molecular dynamics (MD) studies. The same has been done for the argon copper nanofluid with varying degrees of volume fractions of the nanoparticle.

a. First Validation

First the validation was performed for an argon - copper nanofluid system by using the same configuration of Achhal et al. [34].

System setup:

The system was modelled using a cubic simulation box of size 68.64 Å × 68.64 Å × 68.64 Å. The simulation box is filled with argon atoms arranged in a face-cantered cubic (fcc) lattice with a lattice parameter of 5.72 Å. The time-step used in this simulation is 1 fs.

Force field:

In this simulation, the argon-argon interaction is modelled with L-J potential, using $\sigma_{Ar} = 0.3405\ nm$ & $\varepsilon_{Ar} = 1.66 \times 10^{-21}\ J$.The copper-copper interaction is modelled with L-J potential, using $\sigma_{Cu} = 0.2337\ nm$ & $\varepsilon_{Cu} = 65.625 \times 10^{-21}\ J$ [34]. The argon-copper interaction was obtained using the mixing rule.

Equilibration:

The system was equilibrated first for 2000 picoseconds at 86 K. This equilibration was preformed using an NVT ensemble.

This equilibration was performed to remove any residual forces from the initial configuration and to reach a steady state.

The second equilibration step was performed for 2000 picoseconds also at 86 K. This equilibration was preformed using an NVE ensemble.

Production Run:

After equilibration, the production run was performed for 2000 picoseconds. The temperature of the system was kept constant via an NVE ensemble, and the heat flux was calculated.

The results of the validation study are shown in the table 4-1 and compared to the results published by Achhal et al. [34]. It should be noted that the results reported by Achhal et al. [34] was obtained using the green-kubo method.

Table 4-1 Results of the validation study & comparison.

Volume fraction % $Cu_{Nanoparticle}$	**Number of Cu_{Atoms}**	**Number of Ar_{Atoms}**	**Radius (Å) of $Cu_{Nanoparticle}$**	**Calculated Thermal conductivity (W/mK)**	**Thermal conductivity (W/mK) by Achhal et al.** [34]	**Percentage Error (%)**
0.19	14	6897	4	0.1419	0.1351	5.03
0.65	80	6877	6	0.2596	0.2155	20.46
1.52	188	6836	8	0.4846	0.4188	15.71
2.93	370	6773	10	0.8718	0.8430	3.416

The percentage error shown in table 4-1 is highly inconsistent. Which is probable given that the thermal conductivity was obtained by two different methods, namely, NEMD direct method and EMD green-kubo method. Refer to section 2.1 “l Choosing the Appropriate Method” for a detailed discussion on the two methods.

b. Second Validation

Second the validation was performed for an ethylene glycol - copper nanofluid system by using the same configuration of Khamliche et al. [31].

System setup:

The system was modelled using a cubic simulation box of size 100 Å × 100 Å × 100 Å. The simulation box is filled with ethylene glycol atoms arranged in a face-cantered cubic (fcc) lattice with a lattice parameter of 5.0553 Å. The time-step used in this simulation is 0.04 fs. The nanoparticle was added in the centre of the box with a diameter of 3 nm.

Force field:

In this simulation, the ethylene glycol interactions are modelled with L-J potential, using the values in the table 4-2 [31].

Table 4-2 LJ parameters for the EG/Cu nanofluid system.

Atom (i-j)	**εij (kcal/mol)**	**σij (Å)**
H-C	0.03	2.5
C-C	0.066	3.5
O-H	0.17	3.07
H-Cu	0.03396	1.335
O-Cu	0.06387	2.7172

And the copper-copper interaction is modelled using embedded atom model (EAM) [16].

The ethylene glycol – copper interaction was obtained using the mixing rule.

Equilibration:

The system was equilibrated first for 100 picoseconds at 298 K. This equilibration was preformed using an NVT ensemble.

This equilibration was performed to remove any residual forces from the initial configuration and to reach a steady state.

The second equilibration step was performed for 100 picoseconds also at 298 K. Th is equilibration was preformed using an NPT ensemble.

Production Run:

After equilibration, the production run was performed for 100 picoseconds. The temperature of the system was kept constant via an NVE ensemble, and the heat flux was calculated.

The thermal conductivity was calculated at 0.2868 W/mK which is in good agreement with the published thermal conductivity of Khamliche et al. [31] at 0.29 W/mK.

4.2Lennard-Jones Parameter Optimisation

The Lennard-Jones (LJ) potential is a simple, yet powerful mathematical model used to describe the pairwise interaction between particles in molecular dynamics simulations. Its importance in computational chemistry and biophysics lies in its ability to capture the key features of intermolecular forces, such as the attractive van der Waals forces and the repulsive forces due to electron cloud overlap. However, the accuracy and reliability of the LJ potential depend on the its parameters, which determine the depth of the potential well and the distance at which the potential is at its minimum.

The optimisation of Lennard-Jones parameters plays a critical role in ensuring accurate and reliable molecular dynamics simulations. The optimised parameters enable researchers to obtain meaningful insights into the behaviour of molecular systems, improve the stability of simulations and facilitation of computational efficiency. Optimised LJ parameters are crucial for accurately representing the interactions between particles in a simulated system. This ensures that the simulation results closely resemble experimental observations and provide reliable insights into the behaviour of the system. Also, properly optimised parameters lead to more stable simulations, reducing the likelihood of numerical instabilities and artifacts. This results in more reliable and consistent outcomes in molecular dynamics studies.

The initial LJ parameters used in the PAO-2/Cu nanofluid system is shown in table 4-3.

Table 4-3 LJ parameters used in the PAO-2/Cu nanofluid system

Atom (i-j)	**εij (kcal/mol)**	**σij (Å)**
C-C	0.066	3.5
H-H	0.026	2.5
C-H	0.0445	2.958
C-Cu	0.31152	2.5
H-Cu	0.03396	1.335

The C-C, H-H, and C-H interactions were obtained from Khamliche et. al [31].
C-Cu and H-Cu interactions were obtained using the mixing rules or combination rules. The combination rules for the Lennard-Jones parameters are used when simulating mixed systems with different types of particles. These combination rules are known as the Lorentz-Berthelot rules:

$$\sigma_{ij} = \frac{\sigma_{ii} + \sigma_{jj}}{2}, \quad 4\text{-}1$$

$$\varepsilon_{ij} = \sqrt{\varepsilon_{ii}\varepsilon_{jj}} \quad 4\text{-}2$$

In the PAO-2/Cu simulations these parameters worked well in keeping the nanoparticle intact during NPT and NVT ensembles. However, it did not result in an accurate density and thermal conductivity of the system.

After further investigation, the problematic H-Cu parameter was identified. Thus, the parameter ε_{HCu} was simulated at different values of 0.043, 0.053, 0.063, 0.073, 0.083, 0.093. The best candidate was identified as $\varepsilon_{HCu} = 0.073$ with density equal to 0.85029685 g/cm^3 at 1% volume fraction of Copper. This is in good agreement with the density of pure PAO oil of 0.8318 g/cm3 [102]. Indeed, the calculated density is slightly higher than the reported PAO oil density due to the presence of copper atoms.

The LJ parameters for the PAO-2/Ag nanofluid system shown in table 4-4, on the other hand, worked perfectly and was obtained from Sarkar et al [102]. Except for the H-H interaction which was obtained from Khamliche et. al [31].

Table 4-4 LJ parameters used in the PAO-2/Ag nanofluid system.

Atom (i-j)	**εij (kcal/mol)**	**σij (Å)**
C-C	0.0665	3.506
H-H	0.03	2.5
C-H	0.030	2.958
C-Ag	0.744	2.9905
H-Cu	0.657	2.316

In conclusion, the LJ potential obtained from the mixing rule used for the C-Cu and H-Cu interactions were not describing the PAO2-Cu system accurately. Thus, an attempt was made through trial and error to get the optimised values for the C-Cu and H-Cu interactions that accurately described the PAO2-Cu system.

4.3Nanofluid Simulations

Two nanofluid systems were prepared to preform thermal conductivity calculations.

The first system consists of PAO-2 base fluid with copper nanoparticle which is 1 nm in diameter.

The second system consists of PAO-2 base fluid with silver nanoparticle which is 1 nm in diameter.

Silver nanoparticle was chosen in the nanofluid due to its unique properties that contribute to enhanced thermal conductivity, heat transfer, and stability. Silver has one of the highest thermal conductivities among metals, which makes it an excellent material for improving the heat transfer efficiency of a base fluid when used as nanoparticles. Silver nanoparticles exhibit good chemical stability in various fluids, ensuring that the nanofluid retains its desired properties over time. The unique properties of silver nanoparticles make them suitable for various applications, such as heat exchangers, cooling systems, and electronic devices, where enhanced heat transfer and thermal management are essential. Silver nanoparticles can be easily dispersed in different base fluids, resulting in stable nanofluids with minimal particle agglomeration [103].

In both cases the size of the periodic box is 46.459 x 46.459 x 46.459 Å and consists of 10044 PAO-2 atoms.

The simulations were performed for 5 different volume fractions for each system from 1% to 5% volume fraction.

For the copper nanoparticle the volume fractions of 1%, 2%, 3%, 4%, and 5% translates to 133, 265, 398, 530, and 648 copper atoms respectively.

For the silver nanoparticle the volume fractions of 1%, 2%, 3%, 4%, and 5% translates to 80, 160, 239, 319, and 399 silver atoms respectively.

The periodic box is partitioned into 46 sections along the z-direction. The first through third sections function as the heat source, whereas the twenty-third through twenty-sixth sections serve as the heat sink region.

The system was equilibrated under NPT ensemble for 2,000,000 timesteps, followed by 2,000,000 timesteps in the NVT ensemble, where the timestep is equal to 0.5 fs. Subsequently

under NVE ensemble, during the next 4,000,000 timesteps, a consistent heat flux is applied in the z-direction by simultaneously adding energy (0.0001 kcal/mol) to the heat source region and removing an equivalent amount of energy from the heat sink region over equal time intervals. First and last timesteps of the simulation box is shown in the figures below.

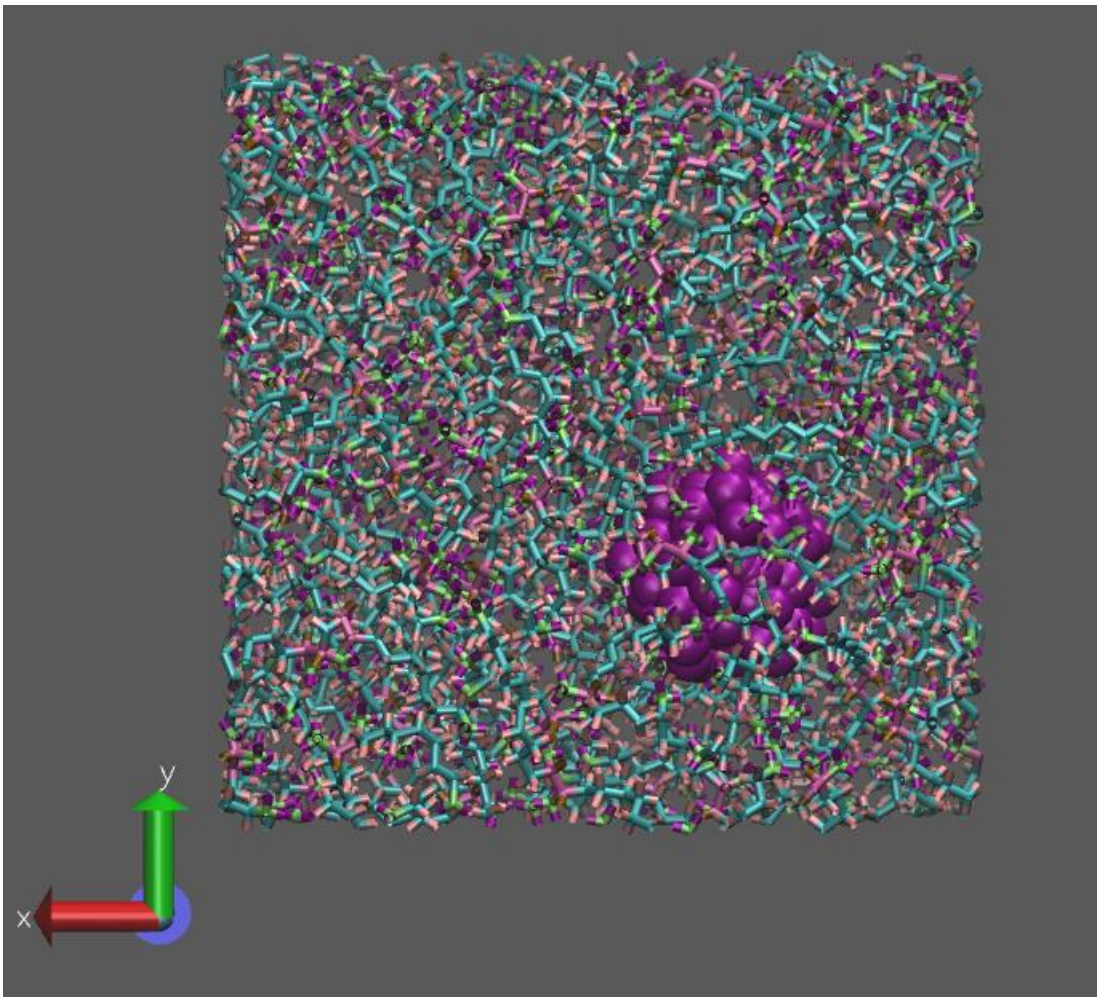

Figure 4-1 First timestep after minimisation: Copper NP.

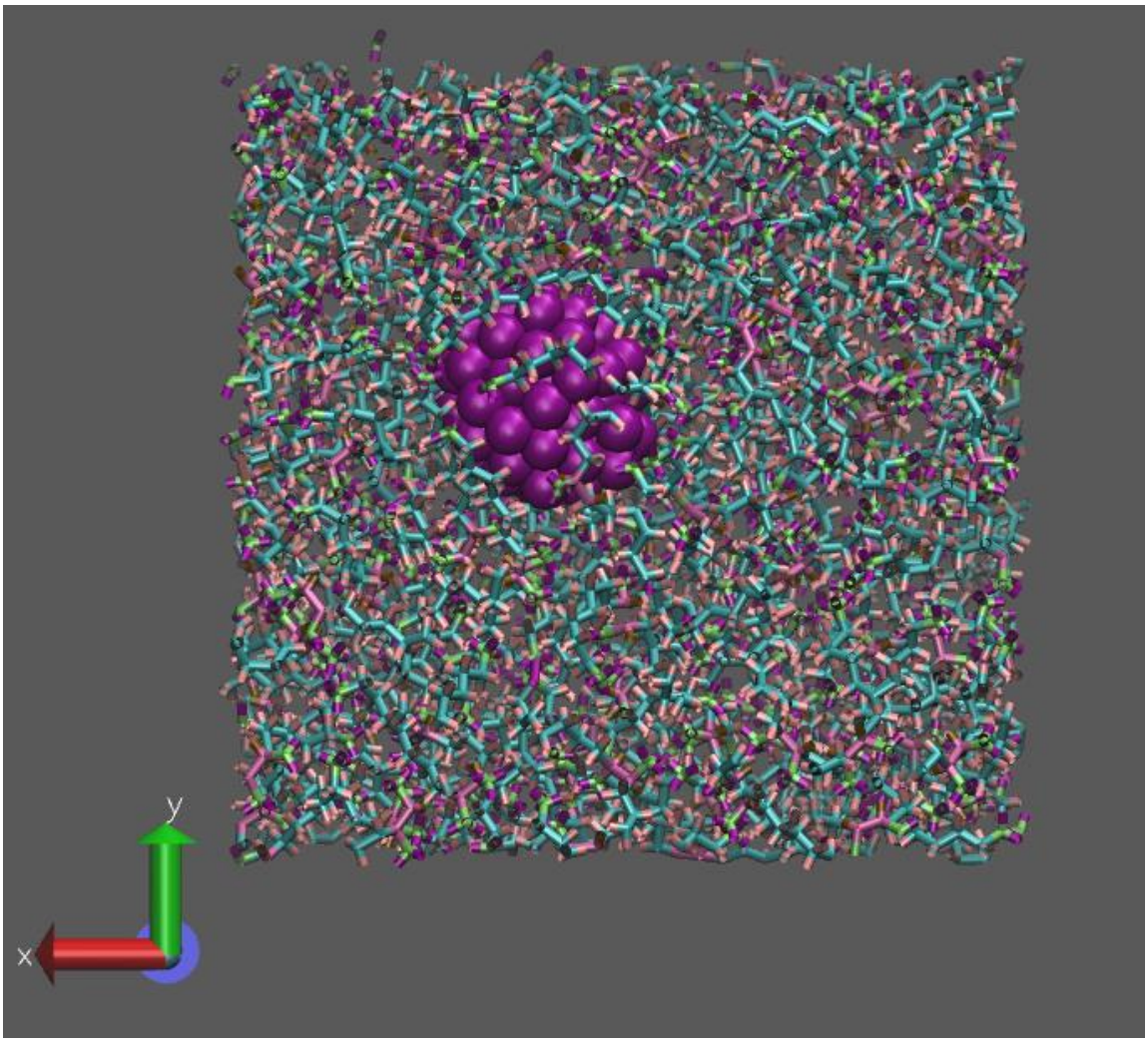

Figure 4-2 Last timestep of the production run: Copper NP.

As you can see in Figure 4-2 the nanoparticle kept its shape and stayed intact throughout the simulation.

4.4Thermal Conductivity

The result of the PAO-2 base fluid thermal conductivity was obtained through MD simulation using the same methodology described in section 3.

The calculated thermal conductivity at temperature 293 K is shown in Figure 4-3.

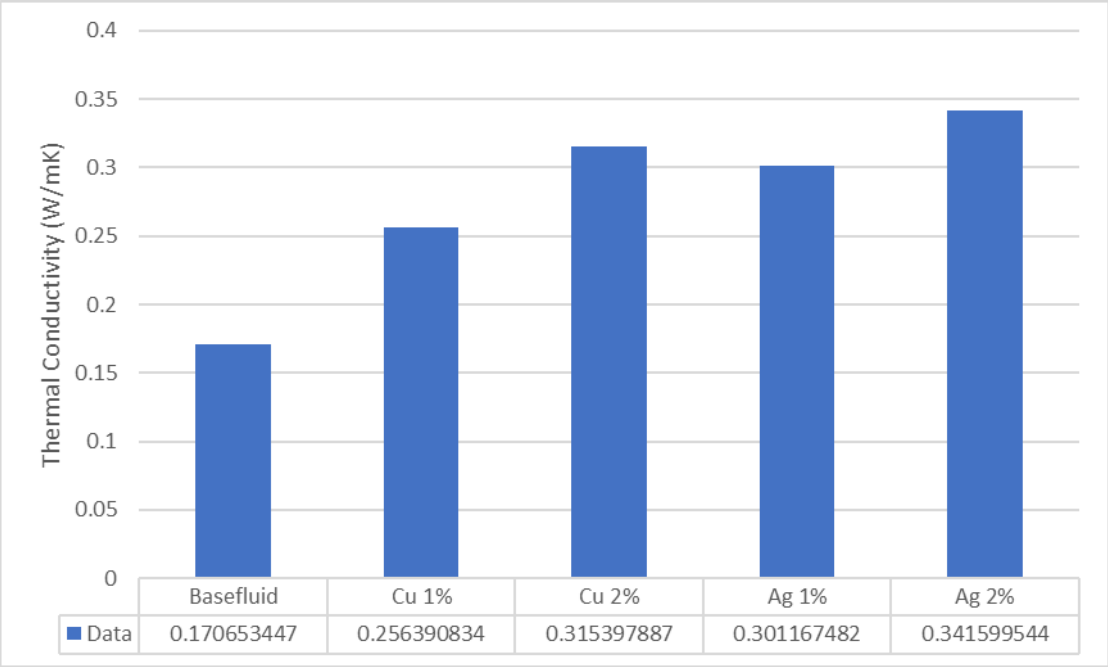

Figure 4-3 Calculated thermal conductivity at 293 K.

The calculated thermal conductivity enhancement of PAO2/Cu and PAO2/Ag nanofluids at volume fraction of 1% and 2% at temperature of 293 K is shown in table 4-5.

The thermal conductivity enhancement of the PAO2/Ag is noticeably higher than that of PAO2/Cu at the two different volume fractions. This result is logical and expected since the thermal conductivity of the silver is higher than copper and has one of the highest thermal conductivities amongst metals.

Table 4-5: Thermal conductivity enhancement of PAO2/Cu and PAO2/Ag.

Nanofluid	Nanoparticle vol. fraction (%)	Nanofluid Thermal conductivity (W/mK)	Base fluid thermal conductivity (W/mK)	Enhancement (%)
PAO-2/Cu	1	0.2563	0.1706	50%
PAO-2/Ag	1	0.3011	0.1706	76%
PAO-2/Cu	2	0.3153	0.1706	84%
PAO-2/Ag	2	0.3415	0.1706	100%

Since data regarding the properties PAO-2 is limited in literature, the base fluid thermal conductivity of PAO-2 at 0.1706 W/mK is compared to the thermal conductivity of PAO at 0.143 W/mK according to Xu et al [104].

Also, there are no studies to date that explore PAO-2 nanofluids. Thus, the calculated thermal conductivity was compared to comparable base fluids like ethylene glycol and oil.

The calculated results for 1% volume fraction of copper shows significant thermal conductivity enhancement of 50% compared to 15% thermal conductivity enhancement of 1% volume fraction of copper in ethylene glycol base fluid, where the ethylene glycol base fluid thermal conductivity is 0.252 W/mK and the nanofluid thermal conductivity is 0.29 W/mK [31].

Another comparison can be made to the experimental study of engine oil/Cu nanofluid by Aberoumand et al [105]. They reported 16% thermal conductivity enhancement of engine oil/Cu nanofluid, where the engine oil base fluid thermal conductivity is 0.13 W/mK and the thermal conductivity of the nanofluid at 1% volume fraction of copper is 0.152 W/mK.

Extra comparison can be made to the experimental study of mineral oil/Cu nanofluid by Esfahani et al. [106].They reported 8% thermal conductivity enhancement of mineral oil/Cu nanofluid, where the mineral oil base fluid thermal conductivity is 0.157 W/mK and the thermal conductivity of the nanofluid at 0.05% volume fraction of copper is 0.17 W/mK.

Thus, the PAO-2/Cu nanofluid at 1% volume fraction of copper shows significant enhancement in thermal conductivity and would be a good candidate for heat transfer liquid for BTMS.

As mentioned earlier, silver nanoparticle was chosen for its enhanced thermal conductivity and that was reflected in the 76% thermal conductivity enhancement. However, this type of nanofluid wasn't explored in literature, thus it is difficult to compare the results.

Overview of the discussed comparison is shown in table 4-6.

Table 4-6: Comparison of thermal conductivity enhancement.

Base fluid	**Base fluid thermal conductivity (W/mK)**	**Nanofluid (1% vol. fraction of Cu)**	**Nanofluid Thermal conductivity (W/mK)**	**Enhancement (%)**	**Reference**
PAO-2	0.1706	PAO-2/Cu	0.2559	50	Own calculation
Ethylene glycol	0.252	Ethylene glycol/Cu	0.29	15	[31]
Engine oil	0.13	Engine oil/Cu	0.152	16	[105]
Mineral oil	0.157	Mineral oil/Cu (0.05% vol. fraction of Cu)	0.17	8	[106]

Refer to section 2.5 on a discussion of the importance and impact of enhanced thermal conductivity of nanofluids on BTMS.

5. Conclusions

In this thesis, the potential of nanofluids for electric car battery cooling systems was investigated through Molecular Dynamics (MD) simulations. The study focused on exploring the thermal properties of nanofluids and provided valuable insights into the design and optimization of heat transfer fluids for electric car battery cooling systems. Two nanofluid systems were studied, with one consisting of a PAO-2 base fluid with copper nanoparticles, and the other with silver nanoparticles.

The results of this study demonstrated a significant enhancement in thermal conductivity for both nanofluid systems. The PAO-2/Cu nanofluid at 1% volume fraction of copper showed a 50% enhancement in thermal conductivity, while the PAO-2/Ag nanofluid at 1% volume fraction of silver showed a 76% enhancement. These enhancements in thermal conductivity indicate that both nanofluids are promising candidates for use in electric car battery cooling systems. Moreover, this study identified crucial factors that impact the thermal conductivity of nanofluids and highlighted the importance of optimizing Lennard-Jones parameters for accurate and reliable MD simulations.

In conclusion, the use of Molecular Dynamics simulations has proven to be an invaluable tool for understanding the complex thermal and transport properties of nanofluids, leading to the identification of potential solutions for improving the performance and longevity of electric car batteries. This study paves the way for future research on the optimization of nanofluids and their application in Battery Thermal Management Systems, contributing to the advancement of electric vehicle technology.

6. Future Work

I hope to continue working on this research at a PhD level, and of course these recommendations are for anyone who would like to work in this area.

The findings of this study provide valuable insights into the potential of nanofluids for enhancing the thermal performance of electric car battery cooling systems. Molecular dynamics simulations have revealed the enhanced thermal conductivity of PAO-2/Cu and PAO-2/Ag nanofluids, demonstrating their potential for application in Battery Thermal Management Systems (BTMS). However, there are several avenues for future research that could further advance our understanding of nanofluids and their application in electric car battery cooling systems.

- Investigation of other nanoparticles:

While this study focused on copper and silver nanoparticles, future research could explore the potential of other metal, such as aluminium, graphene, or carbon nanotubes, for enhancing the thermal performance of nanofluids. This would allow for a broader understanding of the range of materials that can be utilized to improve the thermal properties of heat transfer fluids.

Also, the use of hybrid nanoparticles of different metals and size/shape configurations can be explored to design a nanofluid with optimized thermal and rheological properties.

- Study of nanoparticle shape and size effects:

The influence of nanoparticle shape and size on the thermal conductivity of nanofluids could be investigated. This would provide insights into the optimal nanoparticle characteristics for achieving maximum thermal performance in BTMS applications.

- Study of nanofluids at different temperature

While this study focused on studying the thermal conductivity at 293 K, the effect on the thermal conductivity enhancement should be explored at different temperatures.

- Experimental validation:

Experimental studies could be conducted to validate the findings of the molecular dynamics simulations and to assess the real-world performance of the proposed nanofluid-based BTMS solutions.

- Environmental impact

The environmental impact should be considered when comparing between the best nanofluids candidates. The production and synthesis of nanoparticles may involve the use of hazardous chemicals and energy-intensive processes. The energy required for production and the waste generated can contribute to environmental pollution and greenhouse gas emissions.

By addressing these areas in future research, we can build upon the findings of this thesis and further advance our understanding of nanofluids for electric car battery cooling systems, ultimately contributing to the development of more efficient and sustainable transportation solutions.

7. References

[1] Y. Deng *et al.*, "Effects of different coolants and cooling strategies on the cooling performance of the power lithium ion battery system: A review," *Applied Thermal Engineering*, vol. 142. Elsevier Ltd, pp. 10–29, Sep. 01, 2018. doi: 10.1016/j.applthermaleng.2018.06.043.

[2] M. Lu, X. Zhang, J. Ji, X. Xu, and Y. Zhang, "Research progress on power battery cooling technology for electric vehicles," *J Energy Storage*, vol. 27, p. 101155, Feb. 2020, doi: 10.1016/J.EST.2019.101155.

[3] R. W. Van Gils, D. Danilov, P. H. L. Notten, M. F. M. Speetjens, and H. Nijmeijer, "Battery thermal management by boiling heat-transfer," *Energy Convers Manag*, vol. 79, pp. 9–17, Mar. 2014, doi: 10.1016/J.ENCONMAN.2013.12.006.

[4] C. Roe *et al.*, "Immersion cooling for lithium-ion batteries – A review," *J Power Sources*, vol. 525, p. 231094, Mar. 2022, doi: 10.1016/J.JPOWSOUR.2022.231094.

[5] S. Antoun, S. Srinivasan, and M. Z. Saghir, "A Refined Molecular Dynamics Approach to Predict the Thermophysical Properties of Positively Charged Alumina Nanoparticles Suspended in Water," *International Journal of Thermofluids*, vol. 12, p. 100114, Nov. 2021, doi: 10.1016/J.IJFT.2021.100114.

[6] X. Yin, M. Bai, C. Hu, and J. Lv, "Molecular dynamics simulation on the effect of nanoparticle deposition and nondeposition on the nanofluid explosive boiling heat transfer," *Numeri Heat Transf A Appl*, vol. 73, no. 8, pp. 553–564, Apr. 2018, doi: 10.1080/10407782.2018.1459135.

[7] X. Yin, C. Hu, M. Bai, and J. Lv, "An investigation on the heat transfer characteristics of nanofluids in flow boiling by molecular dynamics simulations," *Int J Heat Mass Transf*, vol. 162, p. 120338, Dec. 2020, doi: 10.1016/J.IJHEATMASSTRANSFER.2020.120338.

[8] H. Kang, Y. Zhang, and M. Yang, "Molecular dynamics simulation of thermal conductivity of Cu-Ar nanofluid using EAM potential for Cu-Cu interactions," *Appl Phys A Mater Sci Process*, vol. 103, no. 4, pp. 1001–1008, Jun. 2011, doi: 10.1007/S00339-011-6379-Z/METRICS.

[9] M. K. Bushehri, A. Mohebbi, and H. H. Rafsanjani, "Prediction of thermal conductivity and viscosity of nanofluids by molecular dynamics simulation," *Journal of Engineering Thermophysics*, vol. 25, no. 3, pp. 389–400, Jul. 2016, doi: 10.1134/S1810232816030085/METRICS.

[10] W. Cui, Z. Shen, J. Yang, S. Wu, and M. Bai, "Influence of nanoparticle properties on the thermal conductivity of nanofluids by molecular dynamics simulation," *RSC Adv*, vol. 4, no. 98, pp. 55580–55589, Oct. 2014, doi: 10.1039/C4RA07736A.

[11] S. Sarkar and R. P. Selvam, "Molecular dynamics simulation of effective thermal conductivity and study of enhanced thermal transport mechanism in nanofluids," *J Appl Phys*, vol. 102, no. 7, p. 074302, Oct. 2007, doi: 10.1063/1.2785009.

[12] M. J. Buehler, "Atomistic modeling of materials failure," *Atomistic Modeling of Materials Failure*, pp. 1–488, 2008, doi: 10.1007/978-0-387-76426-9/COVER.

[13] G. S. Camprubí, *Mechanical properties at nano-level*. Lund University, 2011.

[14] B.J. Alder and T.E. Wainwright, *Molecular Motions*. 1959.

[15] Y. Mishin, M. J. Mehl, D. A. Papaconstantopoulos, A. F. Voter, and J. D. Kress, "Structural stability and lattice defects in copper: Ab initio, tight-binding, and embedded-atom calculations," *Phys Rev B*, vol. 63, no. 22, p. 224106, May 2001, doi: 10.1103/PhysRevB.63.224106.

[16] S. M. Foiles, M. I. Baskes, and M. S. Daw, "Embedded-atom-method functions for the fcc metals Cu, Ag, Au, Ni, Pd, Pt, and their alloys," *Phys Rev B*, vol. 33, no. 12, p. 7983, Jun. 1986, doi: 10.1103/PhysRevB.33.7983.

[17] M. P. Allen and D. J. Tildesley, "Computer Simulation of Liquids," *Computer Simulation of Liquids: Second Edition*, pp. 1–626, Nov. 2017, doi: 10.1093/OSO/9780198803195.001.0001.

[18] L. Verlet, "Computer 'Experiments' on Classical Fluids. I. Thermodynamical Properties of Lennard-Jones Molecules," *Physical Review*, vol. 159, no. 1, p. 98, Jul. 1967, doi: 10.1103/PhysRev.159.98.

[19] W. Liu, B. Schmidt, G. Voss, and W. Müller-Wittig, "Molecular dynamics simulations on commodity GPUs with CUDA," *Lecture Notes in Computer Science (including subseries Lecture Notes in Artificial Intelligence and Lecture Notes in Bioinformatics)*, vol. 4873 LNCS, pp. 185–196, 2007, doi: 10.1007/978-3-540-77220-0_20/COVER.

[20] D. Frenkel and B. Smit, "Understanding Molecular Simulation: Monte Carlo Simulations in Various Ensembles," *Academic Press, London*, pp. 111–137, 2002, Accessed: Sep. 16, 2023. [Online]. Available: https://www.sciencedirect.com/science/article/pii/B9780122673511500079

[21] Z. Liang, W. Evans, and P. Keblinski, "Equilibrium and nonequilibrium molecular dynamics simulations of thermal conductance at solid-gas interfaces," *Phys Rev E Stat Nonlin Soft Matter Phys*, vol. 87, no. 2, p. 022119, Feb. 2013, doi: 10.1103/PHYSREVE.87.022119/FIGURES/8/MEDIUM.

[22] F. Müller-Plathe, "A simple nonequilibrium molecular dynamics method for calculating the thermal conductivity," *J Chem Phys*, vol. 106, no. 14, p. 6082, Aug. 1998, doi: 10.1063/1.473271.

[23] K. Zhou and B. Liu, *Molecular Dynamics Simulation: Fundamentals and Applications*. Elsevier, 2022. doi: 10.1016/B978-0-12-816419-8.00001-5.

[24] Z. Wang, S. Safarkhani, G. Lin, and X. Ruan, "Uncertainty quantification of thermal conductivities from equilibrium molecular dynamics simulations," *Int J Heat Mass Transf*, vol. 112, pp. 267–278, Sep. 2017, doi: 10.1016/J.IJHEATMASSTRANSFER.2017.04.077.

[25] S. G. Volz and G. Chen, "Molecular-dynamics simulation of thermal conductivity of silicon crystals," *Phys Rev B*, vol. 61, no. 4, p. 2651, Jan. 2000, doi: 10.1103/PhysRevB.61.2651.

[26] J. Che, T. Çağin, and W. A. Goddard, "Thermal conductivity of carbon nanotubes," *Nanotechnology*, vol. 11, no. 2, p. 65, Jun. 2000, doi: 10.1088/0957-4484/11/2/305.

[27] J. Che, T. Çağin, W. Deng, and W. A. Goddard, "Thermal conductivity of diamond and related materials from molecular dynamics simulations," *J Chem Phys*, vol. 113, no. 16, p. 6888, Oct. 2000, doi: 10.1063/1.1310223.

[28] P. K. Schelling, S. R. Phillpot, and P. Keblinski, "Comparison of atomic-level simulation methods for computing thermal conductivity," *Phys Rev B*, vol. 65, no. 14, p. 144306, Apr. 2002, doi: 10.1103/PhysRevB.65.144306.

[29] M. Nejatolahi, A. A. Golneshan, R. Kamali, and S. Sabbaghi, "Nonequilibrium versus equilibrium molecular dynamics for calculating the thermal conductivity of nanofluids," *J Therm Anal Calorim*, vol. 144, no. 4, pp. 1467–1481, May 2021, doi: 10.1007/S10973-020-09595-X/METRICS.

[30] Y. Li, Y. Zhai, M. Ma, Z. Xuan, and H. Wang, "Using molecular dynamics simulations to investigate the effect of the interfacial nanolayer structure on enhancing the viscosity and thermal conductivity of nanofluids," *International Communications in Heat and Mass Transfer*, vol. 122, p. 105181, Mar. 2021, doi: 10.1016/J.ICHEATMASSTRANSFER.2021.105181.

[31] T. Khamliche, S. Khamlich, M. K. Moodley, B. M. Mothudi, M. Henini, and M. Maaza, "Laser fabrication of Cu nanoparticles based nanofluid with enhanced thermal conductivity: Experimental and molecular dynamics studies," *J Mol Liq*, vol. 323, p. 114975, Feb. 2021, doi: 10.1016/J.MOLLIQ.2020.114975.

[32] L. Zhou, J. Zhu, Y. Zhao, and H. Ma, "A molecular dynamics study on thermal conductivity enhancement mechanism of nanofluids – Effect of nanoparticle aggregation," *Int J Heat Mass Transf*, vol. 183, p. 122124, Feb. 2022, doi: 10.1016/J.IJHEATMASSTRANSFER.2021.122124.

[33] J. Chen, K. Han, S. Wang, X. Liu, P. Wang, and J. Chen, "Investigation of enhanced thermal properties of CuAr nanofluids by reverse non equilibrium molecular dynamics method," *Powder Technol*, vol. 356, pp. 559–565, Nov. 2019, doi: 10.1016/J.POWTEC.2019.08.051.

[34] E. M. Achhal, H. Jabraoui, S. Zeroual, H. Loulijat, A. Hasnaoui, and S. Ouaskit, "Modeling and simulations of nanofluids using classical molecular dynamics: Particle size

and temperature effects on thermal conductivity," *Advanced Powder Technology*, vol. 29, no. 10, pp. 2434–2439, Oct. 2018, doi: 10.1016/J.APT.2018.06.023.

[35] J. Yu and J. G. Amar, "Effects of Short-Range Attraction in Metal Epitaxial Growth," *Phys Rev Lett*, vol. 89, no. 28, p. 286103, Dec. 2002, doi: 10.1103/PHYSREVLETT.89.286103/FIGURES/5/MEDIUM.

[36] M. Chandrasekar and S. Suresh, "A Review on the Mechanisms of Heat Transport in Nanofluids," *http://dx.doi.org/10.1080/01457630902972744*, vol. 30, no. 14, pp. 1136–1150, Dec. 2010, doi: 10.1080/01457630902972744.

[37] P. Keblinski, S. R. Phillpot, S. U. S. Choi, and J. A. Eastman, "Mechanisms of heat flow in suspensions of nano-sized particles (nanofluids)," *Int J Heat Mass Transf*, vol. 45, no. 4, pp. 855–863, Dec. 2001, doi: 10.1016/S0017-9310(01)00175-2.

[38] J.-H. Lee, S.-H. Lee, C. J. Choi, S. Pil Jang, and S. U. S. Choi, "A Review of Thermal Conductivity Data, Mechanisms and Models for Nanofluids," *Int J Micronano Scale Transp*, vol. 1, no. 4, pp. 269–322, Dec. 2010, doi: 10.1260/1759-3093.1.4.269.

[39] S. P. Jang and S. U. S. Choi, "Role of Brownian motion in the enhanced thermal conductivity of nanofluids," *Appl Phys Lett*, vol. 84, no. 21, pp. 4316–4318, May 2004, doi: 10.1063/1.1756684.

[40] R. Prasher, P. Bhattacharya, and P. E. Phelan, "Thermal conductivity of nanoscale colloidal solutions (nanofluids)," *Phys Rev Lett*, vol. 94, no. 2, p. 025901, Jan. 2005, doi: 10.1103/PHYSREVLETT.94.025901/FIGURES/3/MEDIUM.

[41] A. Einstein, "Investigations on the Theory of the Brownian Movement," *Dover, New York* , 1956.

[42] P. Keblinski, D. G. Cahill, S. K. Das, T. Sundararajan, T. Pradeep, and H. E. Patel, "Comment on 'Model for Heat Conduction in Nanofluids,'" *Phys Rev Lett*, vol. 95, no. 20, p. 209401, Nov. 2005, doi: 10.1103/PhysRevLett.95.209401.

[43] R. Prasher, P. Bhattacharya, and P. E. Phelan, "Thermal conductivity of nanoscale colloidal solutions (nanofluids)," *Phys Rev Lett*, vol. 94, no. 2, p. 025901, Jan. 2005, doi: 10.1103/PHYSREVLETT.94.025901/FIGURES/3/MEDIUM.

[44] P. Bhattacharya, S. K. Saha, A. Yadav, P. E. Phelan, and R. S. Prasher, "Brownian dynamics simulation to determine the effective thermal conductivity of nanofluids," *J Appl Phys*, vol. 95, no. 11 I, pp. 6492–6494, Jun. 2004, doi: 10.1063/1.1736319.

[45] J. Wang, G. Chan, and Z. Zhang, "A Model of Nanofluids Thermal Conductivity," *Proceedings of the ASME Summer Heat Transfer Conference*, vol. 1, pp. 501–508, Mar. 2005, doi: 10.1115/HT2005-72797.

[46] B. J. Alder and T. E. Wainwright, "Velocity autocorrelations for hard spheres," *Phys Rev Lett*, vol. 18, no. 23, pp. 988–990, 1967, doi: 10.1103/PHYSREVLETT.18.988.

[47] Y. Xuan, Q. Li, and W. Hu, "Aggregation structure and thermal conductivity of nanofluids," *AIChE Journal*, vol. 49, no. 4, pp. 1038–1043, Apr. 2003, doi: 10.1002/AIC.690490420.

[48] B. Yang, "Thermal conductivity equations based on Brownian motion in suspensions of nanoparticles (nanofluids)," *J Heat Transfer*, vol. 130, no. 4, Apr. 2008, doi: 10.1115/1.2789721.

[49] J. Eapen *et al.*, "Mean-field versus microconvection effects in nanofluid thermal conduction," *Phys Rev Lett*, vol. 99, no. 9, p. 095901, Aug. 2007, doi: 10.1103/PHYSREVLETT.99.095901/FIGURES/2/MEDIUM.

[50] W. Evans, J. Fish, and P. Keblinski, "Role of Brownian motion hydrodynamics on nanofluid thermal conductivity," *Appl Phys Lett*, vol. 88, no. 9, p. 093116, Mar. 2006, doi: 10.1063/1.2179118.

[51] P. J. Lu, E. Zaccarelli, F. Ciulla, A. B. Schofield, F. Sciortino, and D. A. Weitz, "Gelation of particles with short-range attraction," *Nature 2008 453:7194*, vol. 453, no. 7194, pp. 499–503, May 2008, doi: 10.1038/nature06931.

[52] P. J. Lu, J. C. Conrad, H. M. Wyss, A. B. Schofield, and D. A. Weitz, "Fluids of clusters in attractive colloids," *Phys Rev Lett*, vol. 96, no. 2, p. 028306, Jan. 2006, doi: 10.1103/PHYSREVLETT.96.028306/FIGURES/4/MEDIUM.

[53] E. Zaccarelli, P. J. Lu, F. Ciulla, D. A. Weitz, and F. Sciortino, "Gelation as arrested phase separation in short-ranged attractive colloid–polymer mixtures," *Journal of Physics: Condensed Matter*, vol. 20, no. 49, p. 494242, Nov. 2008, doi: 10.1088/0953-8984/20/49/494242.

[54] R. Prasher, P. E. Phelan, and P. Bhattacharya, "Effect of aggregation kinetics on the thermal conductivity of nanoscale colloidal solutions (nanofluid)," *Nano Lett*, vol. 6, no. 7, pp. 1529–1534, Jul. 2006, doi: 10.1021/NL060992S/ASSET/IMAGES/MEDIUM/NL060992SN00001.GIF.

[55] N. R. Karthikeyan, J. Philip, and B. Raj, "Effect of clustering on the thermal conductivity of nanofluids," *Mater Chem Phys*, vol. 109, no. 1, pp. 50–55, May 2008, doi: 10.1016/J.MATCHEMPHYS.2007.10.029.

[56] J. Philip, P. D. Shima, and B. Raj, "Evidence for enhanced thermal conduction through percolating structures in nanofluids," *Nanotechnology*, vol. 19, no. 30, p. 305706, Jun. 2008, doi: 10.1088/0957-4484/19/30/305706.

[57] H. Zhu, C. Zhang, S. Liu, Y. Tang, and Y. Yin, "Effects of nanoparticle clustering and alignment on thermal conductivities of Fe3O4 aqueous nanofluids," *Appl Phys Lett*, vol. 89, no. 2, p. 023123, Jul. 2006, doi: 10.1063/1.2221905.

[58] J. A. Eastman, S. R. Phillpot, S. U. S. Choi, and P. Keblinski, “Thermal Transport in Nanofluids,” *https://doi.org/10.1146/annurev.matsci.34.052803.090621*, vol. 34, pp. 219–246, Jul. 2004, doi: 10.1146/ANNUREV.MATSCI.34.052803.090621.

[59] L. Xue, P. Keblinski, S. R. Phillpot, S. U. S. Choi, and J. A. Eastman, “Effect of liquid layering at the liquid-solid interface on thermal transport,” *Int J Heat Mass Transf*, vol. 47, no. 19–20, pp. 4277–4284, Sep. 2004, doi: 10.1016/J.IJHEATMASSTRANSFER.2004.05.016.

[60] G. Chen, “Nanoscale Energy Transport and Conversion a Parallel Treatment of Electrons, Molecules, Phonons and Photons,” *Oxford University Press*, 2005.

[61] A. J. Minnich *et al.*, “Thermal conductivity spectroscopy technique to measure phonon mean free paths,” *Phys Rev Lett*, vol. 107, no. 9, p. 095901, Aug. 2011, doi: 10.1103/PHYSREVLETT.107.095901/FIGURES/3/MEDIUM.

[62] G. Chen, “Size and Interface Effects on Thermal Conductivity of Superlattices and Periodic Thin-Film Structures,” *J Heat Transfer*, vol. 119, no. 2, pp. 220–229, May 1997, doi: 10.1115/1.2824212.

[63] D. H. Kumar, H. E. Patel, V. R. R. Kumar, T. Sundararajan, T. Pradeep, and S. K. Das, “Model for heat conduction in nanofluids,” *Phys Rev Lett*, vol. 93, no. 14, p. 144301, Oct. 2004, doi: 10.1103/PHYSREVLETT.93.144301/FIGURES/4/MEDIUM.

[64] J. Buongiorno, “Convective Transport in Nanofluids,” *J Heat Transfer*, vol. 128, no. 3, pp. 240–250, Mar. 2006, doi: 10.1115/1.2150834.

[65] J. Koo and C. Kleinstreuer, “Impact analysis of nanoparticle motion mechanisms on the thermal conductivity of nanofluids,” *International Communications in Heat and Mass Transfer*, vol. 32, no. 9, pp. 1111–1118, Oct. 2005, doi: 10.1016/J.ICHEATMASSTRANSFER.2005.05.014.

[66] G. Domingues, S. Volz, K. Joulain, and J. J. Greffet, “Heat transfer between two nanoparticles through near field interaction,” *Phys Rev Lett*, vol. 94, no. 8, p. 085901, Mar. 2005, doi: 10.1103/PHYSREVLETT.94.085901/FIGURES/3/MEDIUM.

[67] S. Shen, A. Narayanaswamy, and G. Chen, “Surface phonon polaritons mediated energy transfer between nanoscale gaps,” *Nano Lett*, vol. 9, no. 8, pp. 2909–2913, Aug. 2009, doi: 10.1021/NL901208V/SUPPL_FILE/NL901208V_SI_002.PDF.

[68] R. Lenin, P. A. Joy, and C. Bera, “A review of the recent progress on thermal conductivity of nanofluid,” *J Mol Liq*, vol. 338, Sep. 2021, doi: 10.1016/J.MOLLIQ.2021.116929.

[69] B. Barbés, R. Páramo, E. Blanco, and C. Casanova, “Thermal conductivity and specific heat capacity measurements of CuO nanofluids,” *J Therm Anal Calorim*, vol. 115, no. 2, pp. 1883–1891, Feb. 2014, doi: 10.1007/S10973-013-3518-0/FIGURES/10.

[70] R. Agarwal, K. Verma, N. K. Agrawal, R. K. Duchaniya, and R. Singh, “Synthesis, characterization, thermal conductivity and sensitivity of CuO nanofluids,” *Appl Therm*

Eng, vol. 102, pp. 1024–1036, Jun. 2016, doi: 10.1016/J.APPLTHERMALENG.2016.04.051.

[71] X. F. Li, D. S. Zhu, X. J. Wang, N. Wang, J. W. Gao, and H. Li, "Thermal conductivity enhancement dependent pH and chemical surfactant for Cu-H2O nanofluids," *Thermochim Acta*, vol. 469, no. 1–2, pp. 98–103, Mar. 2008, doi: 10.1016/J.TCA.2008.01.008.

[72] G. Paul, J. Philip, B. Raj, P. K. Das, and I. Manna, "Synthesis, characterization, and thermal property measurement of nano-Al95Zn05 dispersed nanofluid prepared by a two-step process," *Int J Heat Mass Transf*, vol. 54, no. 15–16, pp. 3783–3788, Jul. 2011, doi: 10.1016/J.IJHEATMASSTRANSFER.2011.02.044.

[73] R. S. Khedkar, S. S. Sonawane, and K. L. Wasewar, "Water to nanofluids heat transfer in concentric tube heat exchanger: Experimental study," *Procedia Eng*, vol. 51, pp. 318–323, 2013, doi: 10.1016/J.PROENG.2013.01.043.

[74] R. M. Mostafizur, M. H. U. Bhuiyan, R. Saidur, and A. R. Abdul Aziz, "Thermal conductivity variation for methanol based nanofluids," *Int J Heat Mass Transf*, vol. 76, pp. 350–356, 2014, doi: 10.1016/J.IJHEATMASSTRANSFER.2014.04.040.

[75] S. Simpson, A. Schelfhout, C. Golden, and S. Vafaei, "Nanofluid Thermal Conductivity and Effective Parameters," *Applied Sciences 2019, Vol. 9, Page 87*, vol. 9, no. 1, p. 87, Dec. 2018, doi: 10.3390/APP9010087.

[76] D. H. Yoo, K. S. Hong, and H. S. Yang, "Study of thermal conductivity of nanofluids for the application of heat transfer fluids," *Thermochim Acta*, vol. 455, no. 1–2, pp. 66–69, Apr. 2007, doi: 10.1016/J.TCA.2006.12.006.

[77] C. Pang, J. Y. Jung, J. W. Lee, and Y. T. Kang, "Thermal conductivity measurement of methanol-based nanofluids with Al 2O 3 and SiO 2 nanoparticles," *Int J Heat Mass Transf*, vol. 55, no. 21–22, pp. 5597–5602, Oct. 2012, doi: 10.1016/J.IJHEATMASSTRANSFER.2012.05.048.

[78] T. Ambreen and M. H. Kim, "Influence of particle size on the effective thermal conductivity of nanofluids: A critical review," *Appl Energy*, vol. 264, Apr. 2020, doi: 10.1016/J.APENERGY.2020.114684.

[79] X. Wang, X. Xu, and S. U. S. Choi, "Thermal Conductivity of Nanoparticle - Fluid Mixture," *https://doi.org/10.2514/2.6486*, vol. 13, no. 4, pp. 474–480, May 2012, doi: 10.2514/2.6486.

[80] H. E. Patel, T. Sundararajan, and S. K. Das, "An experimental investigation into the thermal conductivity enhancement in oxide and metallic nanofluids," *Journal of Nanoparticle Research*, vol. 12, no. 3, pp. 1015–1031, Mar. 2010, doi: 10.1007/S11051-009-9658-2/TABLES/2.

[81] P. B. Maheshwary, C. C. Handa, and K. R. Nemade, "A comprehensive study of effect of concentration, particle size and particle shape on thermal conductivity of titania/water

based nanofluid," *Appl Therm Eng*, vol. 119, pp. 79–88, 2017, doi: 10.1016/J.APPLTHERMALENG.2017.03.054.

[82] S. M. S. Murshed, K. C. Leong, and C. Yang, "Enhanced thermal conductivity of TiO2 - Water based nanofluids," *International Journal of Thermal Sciences*, vol. 44, no. 4, pp. 367–373, Apr. 2005, doi: 10.1016/J.IJTHERMALSCI.2004.12.005.

[83] L. S. Sundar, M. K. Singh, and A. C. M. Sousa, "Thermal conductivity of ethylene glycol and water mixture based Fe3O4 nanofluid," *International Communications in Heat and Mass Transfer*, vol. 49, pp. 17–24, Dec. 2013, doi: 10.1016/J.ICHEATMASSTRANSFER.2013.08.026.

[84] M. Kole and T. K. Dey, "Role of interfacial layer and clustering on the effective thermal conductivity of CuO-gear oil nanofluids," *Exp Therm Fluid Sci*, vol. 35, no. 7, pp. 1490–1495, Oct. 2011, doi: 10.1016/J.EXPTHERMFLUSCI.2011.06.010.

[85] P. Kumar, D. Chaudhary, P. Varshney, U. Varshney, S. M. Yahya, and Y. Rafat, "Critical review on battery thermal management and role of nanomaterial in heat transfer enhancement for electrical vehicle application," *J Energy Storage*, vol. 32, p. 102003, Dec. 2020, doi: 10.1016/J.EST.2020.102003.

[86] A. P. Thompson *et al.*, "LAMMPS - a flexible simulation tool for particle-based materials modeling at the atomic, meso, and continuum scales," *Comput Phys Commun*, vol. 271, p. 108171, Feb. 2022, doi: 10.1016/J.CPC.2021.108171.

[87] S. Plimpton, "Computational limits of classical molecular dynamics simulations," *Comput Mater Sci*, vol. 4, no. 4, pp. 361–364, Nov. 1995, doi: 10.1016/0927-0256(95)00037-1.

[88] A. I. Jewett *et al.*, "Moltemplate: A Tool for Coarse-Grained Modeling of Complex Biological Matter and Soft Condensed Matter Physics," *J Mol Biol*, vol. 433, no. 11, p. 166841, May 2021, doi: 10.1016/J.JMB.2021.166841.

[89] A. Stukowski, "Visualization and analysis of atomistic simulation data with OVITO–the Open Visualization Tool," *Model Simul Mat Sci Eng*, vol. 18, no. 1, p. 015012, Dec. 2009, doi: 10.1088/0965-0393/18/1/015012.

[90] W. Humphrey, A. Dalke, and K. Schulten, "VMD: Visual molecular dynamics," *J Mol Graph*, vol. 14, no. 1, pp. 33–38, Feb. 1996, doi: 10.1016/0263-7855(96)00018-5.

[91] A. Kohlmeyer, J. Vermaas, and E. Braun, "TopoTools: Release 1.9," 2022, doi: 10.5281/ZENODO.7071898.

[92] R. Benda, J. Bullen, and A. Plomer, "Synthetics basics: Polyalphaolefins — base fluids for high-performance lubricants," *Journal of Synthetic Lubrication*, vol. 13, no. 1, pp. 41–57, Apr. 1996, doi: 10.1002/JSL.3000130105.

[93] Y. S. Ko, W. S. Kwon, M. H. No, and J. H. Yim, "A study on the control of microstructures of polyalphaolefins via cationic polymerization," *Polymer (Korea)*, vol. 39, no. 2, pp. 346–352, Mar. 2015, doi: 10.7317/pk.2015.39.2.346.

[94] S. S. Scheuermann, S. Eibl, and P. Bartl, "Detailed characterisation of isomers present in polyalphaolefin dimer and the effect of isomeric distribution on bulk properties," *Lubrication Science*, vol. 23, no. 5, pp. 221–232, Aug. 2011, doi: 10.1002/LS.151.

[95] D. Mathas *et al.*, "Evaluation of Methods for Viscosity Simulations of Lubricants at Different Temperatures and Pressures: A Case Study on PAO-2," *Tribology Transactions*, vol. 64, no. 6, pp. 1138–1148, 2021, doi: 10.1080/10402004.2021.1922790/SUPPL_FILE/UTRB_A_1922790_SM8999.PDF.

[96] M. J. Robertson, Y. Qian, M. C. Robinson, J. Tirado-Rives, and W. L. Jorgensen, "Development and Testing of the OPLS-AA/M Force Field for RNA," *J Chem Theory Comput*, vol. 15, no. 4, pp. 2734–2742, Apr. 2019, doi: 10.1021/ACS.JCTC.9B00054/SUPPL_FILE/CT9B00054_SI_001.PDF.

[97] S. W. I. Siu, K. Pluhackova, and R. A. Böckmann, "Optimization of the OPLS-AA force field for long hydrocarbons," *J Chem Theory Comput*, vol. 8, no. 4, pp. 1459–1470, Apr. 2012, doi: 10.1021/CT200908R/SUPPL_FILE/CT200908R_SI_001.PDF.

[98] W. L. Jorgensen and J. Tirado-Rives, "Molecular modeling of organic and biomolecular systems using BOSS and MCPRO," *J Comput Chem*, vol. 26, no. 16, pp. 1689–1700, Dec. 2005, doi: 10.1002/JCC.20297.

[99] K. Pluhackova *et al.*, "Extension of the LOPLS-AA Force Field for Alcohols, Esters, and Monoolein Bilayers and its Validation by Neutron Scattering Experiments," *Journal of Physical Chemistry B*, vol. 119, no. 49, pp. 15287–15299, Dec. 2015, doi: 10.1021/ACS.JPCB.5B08569/ASSET/IMAGES/MEDIUM/JP-2015-085692_0011.GIF.

[100] P. Wirnsberger, D. Frenkel, and C. Dellago, "An enhanced version of the heat exchange algorithm with excellent energy conservation properties," *J Chem Phys*, vol. 143, no. 12, p. 124104, Sep. 2015, doi: 10.1063/1.4931597.

[101] T. Ikeshoji and B. Hafskjold, "Non-equilibrium molecular dynamics calculation of heat conduction in liquid and through liquid-gas interface," *http://dx.doi.org/10.1080/00268979400100171*, vol. 81, no. 2, pp. 251–261, Feb. 2006, doi: 10.1080/00268979400100171.

[102] W. Wijanarko, H. Khanmohammadi, and N. Espallargas, "Effect of Steel Hardness and Composition on the Boundary Lubricating Behavior of Low-Viscosity PAO Formulated with Dodecanoic Acid and Ionic Liquid Additives," *Langmuir*, vol. 38, no. 9, p. 2777, Mar. 2022, doi: 10.1021/ACS.LANGMUIR.1C02848.

[103] S. Sarkar and N. K. Ghosh, "Effect of silver nanoparticle volume fraction on thermal conductivity, specific heat and viscosity of ethylene glycol base silver nanofluid: A molecular dynamics investigation," *J Mol Liq*, vol. 378, p. 121635, May 2023, doi: 10.1016/J.MOLLIQ.2023.121635.

[104] S. K. Das, *Nanofluids : science and technology*. Wiley-Interscience, 2008. Accessed: Mar. 27, 2023. [Online]. Available: https://www.wiley.com/en-us/Nanofluids%3A+Science+and+Technology-p-9780470074732

[105] J. Xu, B. Yang, and B. Hammouda, "Thermal conductivity and viscosity of self-assembled alcohol/polyalphaolefin nanoemulsion fluids," *Nanoscale Res Lett*, vol. 6, no. 1, p. 274, 2011, doi: 10.1186/1556-276X-6-274.

[106] S. Aberoumand and A. Jafarimoghaddam, "Experimental study on synthesis, stability, thermal conductivity and viscosity of Cu–engine oil nanofluid," *J Taiwan Inst Chem Eng*, vol. 71, pp. 315–322, Feb. 2017, doi: 10.1016/J.JTICE.2016.12.035.

[107] J. A. Esfahani *et al.*, "Comparison of experimental data, modelling and non-linear regression on transport properties of mineral oil based nanofluids," *Powder Technol*, vol. 317, pp. 458–470, Jul. 2017, doi: 10.1016/J.POWTEC.2017.04.034.